AD-A082 464 CALIFORNIA INST OF TECH PASADENA DIV OF CHEMISTRY A--ETC F/G 7/4
THE ADSORPTION OF FORMIC ACID ON Y ZEOLITES: A NUCLEAR MAGNETIC--ETC(U)
MAR 80 T M DUNCAN, R W VAUGHAN N00014-75-C-0960
UNCLASSIFIED TR-17 NL

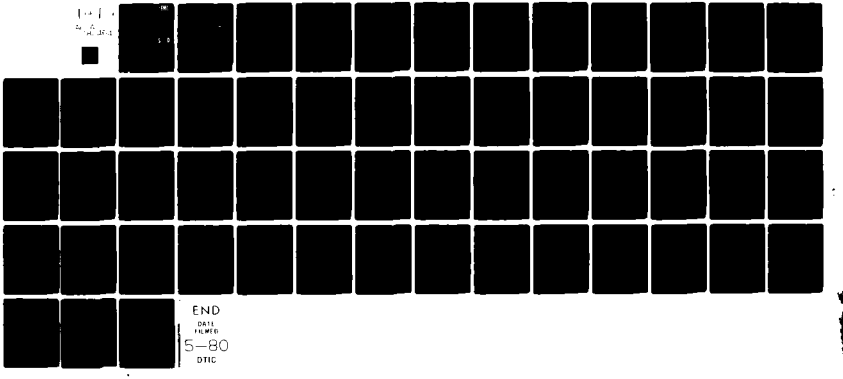

END
DATE FILMED
5-80
DTIC

OFFICE OF NAVAL RESEARCH
Contract N00014-75-C-0960

Technical Report #17

The Adsorption of Formic Acid on Y Zeolites: A Nuclear Magnetic Resonance Study

71

T. M. Duncan and R. W. Vaughan
Division of Chemistry and Chemical Engineering
California Institute of Technology
Pasadena, California 91125

March, 1980

Submitted to the Journal of Catalysis

UNCLASSIFIED

SECURITY CLASSIFICATION OF THIS PAGE (When Data Entered)

REPORT DOCUMENTATION PAGE	READ INSTRUCTIONS BEFORE COMPLETING FORM
1. REPORT NUMBER: Technical Report No. 17 (9)	2. GOVT ACCESSION NO. / 3. RECIPIENT'S CATALOG NUMBER
4. TITLE (and Subtitle): The Adsorption of Formic Acid on Y Zeolites: A Nuclear Magnetic Resonance Study (6)	5. TYPE OF REPORT & PERIOD COVERED
	6. PERFORMING ORG. REPORT NUMBER
7. AUTHOR(s): T. M. Duncan [redacted] R. W. Vaughan (10)	8. CONTRACT OR GRANT NUMBER(s): N00014-75-C-0960 (15)
9. PERFORMING ORGANIZATION NAME AND ADDRESS: California Institute of Technology, Division of Chemistry and Chemical Engineering, Pasadena, California 91125	10. PROGRAM ELEMENT, PROJECT, TASK AREA & WORK UNIT NUMBERS: (12) 57C
11. CONTROLLING OFFICE NAME AND ADDRESS: Office of Naval Research, Chemistry Program Office, Arlington, VA 22217 (11)	12. REPORT DATE: Mar[redacted]80 / 13. NUMBER OF PAGES
14. MONITORING AGENCY NAME & ADDRESS (if different from Controlling Office): (14) TR-17	15. SECURITY CLASS. (of this report): Unclassified / 15a. DECLASSIFICATION/DOWNGRADING SCHEDULE

16. DISTRIBUTION STATEMENT (of this Report)

Approved for Public Release; Distribution Unlimited

17. DISTRIBUTION STATEMENT (of the abstract entered in Block 20, if different from Report)

18. SUPPLEMENTARY NOTES

Preprint; submitted to the Journal of Catalysis

19. KEY WORDS (Continue on reverse side if necessary and identify by block number)

Catalysis, nuclear magnetic resonance, formic acid, zeolites, molecular seives, dehydration reaction

20. ABSTRACT (Continue on reverse side if necessary and identify by block number)

A solid state nuclear magnetic resonance (NMR) study of the adsorption of formic acid on ammonium-Y (NH_4-Y) and ultrastable hydrogen-Y (H-Y) zeolites confirms the results of a previously reported infrared study and provides a further description of the adsorbed states. The formic acid is adsorbed on the NH_4-Y and ultrastable H-Y zeolites in two different forms; as a unidentate formate ligand and as a bidentate formate species, as determined by the sy-metry of the chemical shift powder patterns. Cross-polarization

DD FORM 1 JAN 73 1473 EDITION OF 1 NOV 65 IS OBSOLETE
S/N 0102-LF-014-6601

UNCLASSIFIED 071575

SECURITY CLASSIFICATION OF THIS PAGE (When Data Entered)

techniques exploit the difrerences in ^{13}C-^{1}H dipolar couplings to separate the two groups. The ratio of unidentate to bidentate species is about 52:48 on the NH_4-Y zeolite and about 83:17 on the ultrastable H-Y zeolite. The strength of the ^{13}C-^{27}Al dipolar interaction suggests that the formate ions are directly bonded to the Al atoms of the zeolites. The carbonyl hydrogen, observed by dipolar-difference NMR techniques, is more acidic than that of formic acid, suggesting that the hydrogen is relatively more reactive.

I. INTRODUCTION

The adsorption of formic acid on ammonium-Y (NH_4-Y) and ultrastable hydrogen-Y (H-Y) zeolites has been studied recently by transmission infrared spectroscopy (1). A brief review of the adsorption of formic acid on metal oxides as well as a description of the two zeolites has been discussed previously (1). From the results of the adsorption isotherm and the position of the infrared bands, it was determined that the formic acid was chemically adsorbed on the zeolites as both unidentate formate ligands (species I) and bidentate formate species. Through analogies with other studies of adsorbed formic acid and the infrared spectrum of aluminum formate, it was suggested that the formate ion was bonded to the surface as a bidentate group (species II or III). The infrared spectra

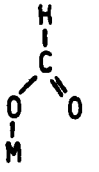

I

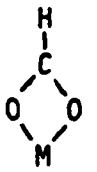

II

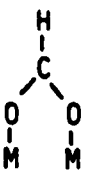

III

indicated that the NH_4-Y sample had a nearly even distribution of the two surface species, whereas the formic acid adsorbed on the ultrastable H-Y sample was present primarily as the formate ion. It has been proposed that the decomposition of the adsorbed formate group is the rate-determining step in the catalytic reaction of formic acid to yield carbon monoxide and water (2). Since the ultrastable H-Y zeolite is more active

catalytically than the NH_4-Y zeolite, the distribution of the surface states of the formic acid has important implications in the role of the configuration of the adsorbed species.

We present here a solid-state nuclear magnetic resonance (NMR) study of the adsorption of formic acid on NH_4-Y and ultrastable H-Y zeolites. The application of NMR technqiues to the study of adsorbed species has been discussed in several reviews (3,4,5). Although there have been numerous NMR studies of physically adsorbed hydrocarbons, there have been relatively few applications to the study of chemically adsorbed species. Examples of chemically adsorbed systems include the study of benzene on charcoal and silica gel (6), carbon dioxide on molecular sieves (7), and carbon monoxide on rhodium on alumina (8). One difficulty with NMR studies of chemisorbed molecules is the extremely weak NMR signals of such dilute systems, which is further complicated by excessive broadening. To date, most studies on physically adsorbed molecules have concentrated on the spin-lattice relaxation times and the isotropic frequency of the resonance. This study will concentrate more on the anisotropic chemical shift tensor and the dipolar interaction of the ^{13}C nuclei with neighboring nuclei, two quantities which are averaged-out in physically adsorbed systems. These quantities will be used to determine the geometry of the adsorbed state, the degree of motion on the surface and the nature of the adsorption site on the substrate.

This study will utilize several high-resolution NMR pulse sequences (9,10,11), including spin-decoupling (12), cross-polarization (12,13), dipolar-modulation (14), and dipolar-difference (15) techniques to enhance the NMR signals and remove the extraneous broadening. The analysis will

be based primarily on ^{13}C NMR spectra. The ^{13}C nuclei are a dilute spin system in the zeolite and interact only through other spin systems or the lattice; thus, there is no broadening from homonuclear interactions. The ^{13}C chemical shifts are much larger than those of ^{1}H nuclei, which allows an interpretation of the spectra even in the presence of substantial broadening. The ^{1}H spectrum of the carbonyl proton of formic acid will be measured also as a cross-reference on the environment of the adsorbed species.

The NMR pulse techniques will be used to measure the chemical shift tensor, the dipolar interactions with ^{1}H and ^{27}Al nuclei, and the various relaxation times of the ^{13}C nuclei of the adsorbed formic acid. The center of mass of the chemical shift tensor (the isotropic value observed in physically adsorbed samples) reflects the general character of the chemistry of the molecular species; that is, the isotropic chemical shift readily distinguishes between fundamentally different carbon compounds such as carbonyl, aliphatic, and aromatic groups. However, the isotropic value is not a good indicator of subtle chemical differences within a subgroup such as the formate compounds (16). Rather, the changes in bonding geometry are better reflected by the anisotropy of the chemical shift tensor. In general, within a subgroup the isotropic value indicates the average electron density at the ^{13}C nucleus, whereas the full tensor is sensitive to changes in the angular distribution and symmetry of the electron density.

The interaction of the ^{13}C nuclei with neighboring dipoles can be used to determine average internuclear distances and the extent of

motional averaging. The ^{13}C nuclei are most strongly coupled to the nuclei of the directly bonded hydrogen atoms. Thus, it is possible to apply cross-polarization techniques to study the strength of the coupling (13) and to enhance the ^{13}C NMR spectrum (12). The interaction may be quantified further by the dipolar-modulation experiment (14). Finally, the dipolar interaction may be used to isolate the ^{1}H NMR spectrum of the carbonyl proton from the broad, diffuse lineshape of the other protons of the sample (15). The extent of the ^{27}Al broadening of the ^{13}C NMR spectrum provides an estimate of the ^{13}C-^{27}Al internuclear distance and, thus, information on the adsorption site of the formic acid.

The three time constants measured in this study are the spin-lattice relaxation time (T_1), the transverse relaxation time (T_2), and the time constant for the coupling between the ^{13}C and ^{1}H spin baths (T_{IS}). The T_1 is the time constant for the rate that the perturbed magnetization returns to equilibrium with the external magnetic field. In samples with relatively high paramagnetic impurity levels, as is the case with the two zeolites studied here, the T_1 of a chemisorbed species cannot be used to determine the nature of the motion on the surface or the cross-relaxation rate with neighboring spins. However, in some cases the T_1 may be used to differentiate between various adsorbed states by the nature of the coupling to the paramagnetic centers (8). T_2 is essentially the lifetime of the state, which is often limited by motions of the molecule or motions of nearby unpaired electrons of paramagnetic centers. T_{IS} is measured by the rate at which the magnetization is transferred between the ^{13}C and the ^{1}H spin systems and may be used to calculate the strength of the

dipolar interaction.

II. EXPERIMENTAL PROCEDURE

A. Sample Description and Preparation

The ammonium-Y (NH_4-Y) zeolite, unit cell formula $Na_2(NH_4)_{48}(AlO_2)_{50}(SiO_2)_{142}\cdot 267H_2O$, was prepared by ion exchange with a sodium-Y zeolite. This NH_4-Y zeolite was calcined at 775 K to yield a "deep bed" product, an ultrastable hydrogen-Y (H-Y) zeolite, with unit cell formula $Na_2H_{48}(AlO_2)_{50}(SiO_2)_{142}\cdot 26H_2O$ (17). The zeolites contain 780 ± 10 ppm Fe and 12 ± 2 ppm Mn, as determined by atomic absorption. The electron paramagnetic spectrum of the zeolites at 8 K and the microwave frequency at 9.25 GHz show a sharp transition at g = 4.4 and a multiplet of about 6 transitions ranging from g = 2.2 to 1.9. The sharp line at g = 4.4 is typical of Fe^{++} in silica-aluminas, whereas the multiplet at about g = 2.0 is indicative of Mn^{++} (18). The sharpness of the transitions indicates that the paramagentic centers are atomically dispersed in the zeolites and not clustered in metallic particles.

The zeolite samples were outgassed with a liquid nitrogen-trapped diffusion pump to pressures of about 5×10^{-5} Torr (1 Torr = 133.3 Nm^{-2}) by heating for 3 hours: the NH_4-Y zeolite at 385 K and the ultrastable H-Y at 800 K. The nitrogen BET surface areas of the zeolites are 459 ± 10 m^2/g and 515 ± 10 m^2/g for the NH_4-Y and the ultrastable H-Y, respectively, representing monolayers of about 63 and 84 nitrogen molecules per unit cell. The formic acid adsorption isotherms for both zeolites, measured previously (1), reveal monolayer coverages of 75 and 56 formic acid molecules per unit for the

NH_4-Y and the ultrastable H-Y, respectively. A submonolayer of isotopically enriched (91.2% ^{13}C) formic acid was deposited on the outgassed NH_4-Y and ultrastable H-Y zeolites by condensation from the gas phase. The predetermined pressure of the vapor to be deposited was calculated from the monomer/dimer equilbrium data of Coolidge (19).

This NMR study was performed on two samples of zeolites with submonolayer coverages of formic acid. Quantitatively, one sample consisted of 0.120 g of NH_4-Y zeolite loaded with 1.81×10^{-4} moles (9.9×10^{20} ^{13}C nuclei), a coverage of 24.9 molecules of formic acid per unit cell of zeolite. The second sample was 0.121 g of ultrastable H-Y zeolite dosed with 1.86×10^{-4} moles (1.02×10^{20} ^{13}C nuclei) of formic acid, a coverage of 18.5 molecules of formic acid per unit cell. We are confident that the structural integrity of the NH_4-Y zeolite is maintained under this light loading of the acid. The acid coverage is significantly below the point where the anomalies occur in the adsorption isotherm and the ratio of hydrogen ions to ammonium ions is low, an important criterion for zeolite stability (20).

The ^{13}C NMR spectra of the reference compounds were obtained from enriched samples of formic acid, ammonium formate, and calcium formate. The formic acid sample was 20% ^{13}C-enriched, prepared by diluting the 91.2% stock with natural abundance formic acid. The ammonium formate sample (12% ^{13}C-enriched) was prepared by neutralizing the formic acid with ammonium formate and then vacuum-desiccating to remove the residual water and ammonia. The calcium formate reference, previously examined elsewhere (14), contained 6% ^{13}C and was doped with Mn^{++} to lower spin-

lattice relaxation times.

B. NMR Spectrometer and Pulse Sequences

The Fourier transform ^{13}C and ^{1}H NMR spectra were measured on a double-resonance multiple-pulse spectrometer (21,22). The 1.32 Tesla Varian magnet is stabilized to about 1 ppm with an external ^{19}F pulsed field-frequency lock. The data were taken with a single coil (5 mm diameter) double-resonance probe tuned for ^{1}H resonance at 56.4 MHz and ^{13}C resonance at 14.2 MHz (22). Temperatures were regulated by a dewared nitrogen flow system.

The ^{13}C NMR spectra in this study were obtained by Fourier transforming the signals observed with three techniques: the 180^{o}-τ-90^{o} (23), ^{13}C-^{1}H cross-polarization (12), and ^{13}C-^{1}H dipolar-modulation (14) experiments. The ^{1}H spectrum of the carbonyl proton was observed by the ^{13}C-^{1}H dipolar-difference experiment (15). These four pulse sequences are diagrammed in Figure 1. The intensities and lineshapes of the NMR spectra as a function of the various parameters of each pulse sequence can be used to describe the adsorbed state and the local environment of the formic acid. The main features of each of the pulse schemes will be discussed here only briefly. More extensive discussions may be found in the reviews mentioned earlier (9,10,11).

The 180^{o}-τ-90^{o} pulse sequence provides a quantitative measure of the number of ^{13}C nuclei in the sample; provided that $T_1 >> \tau$, the sequence is repeated only after waiting a period of at least five T_1's, and the proton irradiation is sufficiently intense to decouple the ^{13}C-^{1}H spins. The criterion for heteronuclear decoupling is that the decoupling field

is greater than both the ^{13}C-^{1}H heteronuclear coupling and the ^{1}H-^{1}H homonuclear spin coupling (10); that is, the Larmor frequency of the protons in the decoupling field must be comparable to the spin-flip rate of the protons caused by both the ^{13}C and other protons. The Larmor frequency of the protons in a holding field of 16 G is 68 KHz. The ^{13}C-^{1}H coupling for a bond length of 1.09 Å is less than 45 KHz at the most intense orientation and averages less than 11 KHz. The square root of the second moment of the ^{1}H spectrum of either the NH_4-Y of ultrastable H-Y zeolites is only about 5.2 KHz at 295 K. Thus, 16 G is sufficient to assure reliable ^{13}C spin counts for the adsorbed formic acid. The intensity of the observed magnetization as a function of τ, the delay between the 180° and 90° pulses, may be used to calculate the T_1 of the ^{13}C nuclei (23). The 180°-τ-90° sequence is alternated with a single 90° pulse, and the successive free induction decays are alternately added and subtracted. This add-subtract mode removes instrumental artifacts during the period immediately after the 90° pulse.

The ^{13}C-^{1}H cross-polarization experiment yields enhanced ^{13}C spectra and quantifies the strength of the heteronuclear interaction by measuring the rate of transfer of magnetization between the two spin systems (12). In general, it is not possible to calibrate the intensity of the signal from the cross-polarization experiment for an inhomogeneous system, such as the formic acid adsorbed on the zeolites, without a knowledge of the distribution of bond lengths and the degree of motional averaging. The cross-polarization process will selectively emphasize the signal from ^{13}C nuclei with stronger couplings to the ^{1}H nuclei. The stronger couplings

may be the result of more ^{1}H spins in the immediate environment (within about 5 Å), ^{13}C-^{1}H bonds at select orientations to the external magnetic field (the interaction is proportional to $(3 \cos^2\theta - 1)$, where θ is the angle between the internuclear bond and the external field), or the ^{13}C-^{1}H bond is not being averaged by motion. For ^{13}C-^{1}H internuclear bonds at orientations where the heteronuclear dipolar coupling is weak (i.e., near 55^{o}), the ^{13}C magnetization must be produced by transfer from intramolecular protons, or ^{13}C-^{13}C homonuclear spin transfer. Both processes are slow and require longer ^{13}C locking fields. Thus, it is not feasible to calculate a priori the intensity of the ^{13}C cross-polarization spectra. It is, however, possible to compare relative single intensities from one sample as a function of the experimental parameters.

The Hartmann-Hahn (24) condition for cross-polarization ($\gamma_H H_H = \gamma_C H_C$, where γ is the gyromagnetic ratio and H is the applied magnetic field) was satisfied with fields of 8.6 G at the proton frequency and 34 G at the carbon frequency. The proton decoupling was 8 G for the reference compounds and 16 G for the formic acid adsorbed on the zeolites. To effect a maximum magnetization transfer, cross-polarization times ranged from 0.1 msec, for the ammonium formate at 295 K, to 8.0 msec for calcium formate at 125 K.

The better signal-to-noise ratios of the ^{13}C spectra from the cross-polarization experiment make it feasible to perform more demanding experiments such as studying the shape and intensity as a function of the cross-polarization time, the echo time, or the dipolar evolution time (14). As described earlier, the intensity of the magnetization as a function of the cross-polarization time is a measure of the strength of the coupling of

the ^{13}C spins to the ^{1}H spins. The signal intensity as a function of the echo time is used to calculate the transverse relaxation rate, T_2.

The ^{13}C-^{1}H dipolar-modulation experiment (14,25) is a variation of the cross-polarization scheme, such that immediately after the ^{13}C spin-locking pulse, a series of eight-pulse cycles (26) are applied to decouple the proton homonuclear interaction while allowing the ^{13}C-^{1}H coupling to remain although it is decreased by a scaling factor of about 0.6. Immediately after the eight-pulse cycles, the ^{1}H decoupling pulse is turned on, which conversely decouples the ^{13}C-^{1}H interaction but not the ^{1}H-^{1}H coupling. For ^{13}C-^{1}H systems with very weak or no couplings, the dipolar-modulated spectra will be similar to the cross-polarization spectra. However, for stronger ^{13}C-^{1}H couplings, the ^{13}C magnetization will oscillate during the eight-pulse sequence at a frequency proportional to the ^{13}C-^{1}H coupling. Thus, the extent of the modulation of the ^{13}C magnetization observed after echo as a function of the duration of the dipolar-modulation sequence is determined by the strength of the ^{13}C-^{1}H coupling. With this technique it is possible in some cases to orient the chemical shift principal axis system in the molecular coordinate system by the rate of modulation of different portions of the ^{13}C powder pattern (14,25). Also, the area of the ^{13}C spectrum will oscillate at a frequency proportional to the average ^{13}C-^{1}H coupling in the sample, thus allowing one to calculate the average ^{13}C-^{1}H bond lengths.

The isolated ^{1}H chemical shift spectrum of the carbonyl hydrogen of the absorbed formic acid may be observed with the dipolar-difference experiment (15). In the dipolar-difference experiment, the homonuclear-

decoupled ^1H spectrum is observed alternately in two environments: first, using the eight-pulse cycle (26) to remove the ^1H-^1H interactions, and second, simultaneously irradiating the proton spins with the eight-pulse cycle while irradiating the ^{13}C nuclei to remove the heteronuclear dipolar coupling to the protons (27). Thus, the first cycle will yield chemical shift spectra from all protons except those directly bonded to ^{13}C nuclei, which will be dipolar broadened into the baseline. In the second cycle, this heteronuclear dipolar broadening is removed and all the protons are observed. Alternately adding and subtracting these two signals yields only the spectrum of the protons directly bonded to the ^{13}C nuclei.

The lines through the spectra were obtained by a nonlinear least-squares fit of a theoretical chemical shift powder pattern (28). The spectra of the reference formates and the 180^o-τ-90^o spectra were convoluted with a Lorentzian broadening function, whereas the cross-polarization spectra were convoluted with a Gaussian broadening function.

III. RESULTS

A. ^{13}C NMR Spectra of Formate Compounds

The anisotropy and resolution of the structure of the ^{13}C NMR spectra of formic acid, ammonium formate, and calcium formate both increased as the temperature of the sample was lowered. This suggests that there are molecular motions in the crystals which are being quenched at lower temperatures. The motions are probably small anisotropic waggings or rockings which cause a local averaging in the ^{13}C NMR powder patterns. In each case, the spectra were recorded at the lowest temperatures experimentally feasible, restricted by the limitations of the equipment and the

temperature dependence of the spin-lattice relaxation times.

The ^{13}C NMR spectra of the reference formates shown in Figure 2 were obtained by ^{13}C-^{1}H cross-polarization and then observing the free induction decay immediately after the ^{13}C spin-locking pulse, while decoupling the protons with 8 G. The principal components of the chemical shift tensors are reported in Table 1. The features in the spectrum for formic acid at 125 K, Figure 2(a), suggest three principal components of the chemical shift tensor, but the data do not fit a theoretical powder pattern lineshape. A least-squares fit, shown by the solid line, follows the upfield component at -92 ppm but clearly misses the downfield shoulder. If the three principal components are fixed at the approximate locations of the shoulders, the computed intensities at the center and downfield components are in error, as shown by the dotted line. The distortion from the theoretical lineshape is probably the result of motion as well as an angular dependence of the ^{13}C-^{1}H cross-polarization rate in a polycrystalline sample. The spectrum in Figure 2(a), obtained by cross-polarizing for 8 msec, is less distorted than the spectra that result with only 0.5 msec of ^{13}C-^{1}H spin contacting or at higher temperatures.

The spectrum for ammonium formate shown in Figure 2(b) is the result of cross-polarizing for 0.1 msec at 185 K. At about 195 K, the proton T_1's lengthened from a few msec to over 10 sec, which indicates that the major relaxation process had halted, probably the rapid reorientation of the ammonium ion. The proton T_1's continue to increase at temperatures below 185 K, which prohibited extended averaging.

The calcium formate ^{13}C NMR spectrum exhibited the most pronounced motional effects of the formates studied. The apparent chemical shift anisotropy increases from about 100 ppm at 295 K to 136 ppm at 125 K. The spectrum shown in Figure 2(c) was obtained by cross-polarizing for 8.0 msec at 125 K. A previous ^{13}C NMR study of a calcium formate single crystal detected two distinct sets of chemical shift components for the crystallographically inequivalent formate ions (16). The resolution in the powder pattern of Figure 2(c) is not sufficient to resolve the two spectra, which are separated by only 5, 3, and 0 ppm at the three principal components.

B. Formic Acid Adsorbed on Zeolites

1. ^{13}C T_1 Measurements

The logarithm of the calibrated amplitude of the observed ^{13}C magnetization versus the delay between the 180° and 90° pulses is plotted in Figure 3. If the recovery of the longitudinal magnetization was described by a single T_1, the data would lie on a straight line when plotted as in Figure 3. The curves through these data, however, can be fit with the sum of two exponentials:

$$\text{HCOOH on } NH_4\text{-Y: } M(\tau) = 8.8 \times 10^{19} \left(0.35e^{-\tau/2.6} + 0.65e^{-\tau/82}\right) \quad (1)$$

$$\text{HCOOH on ultrastable H-Y: } M(\tau) = 5.2 \times 10^{19}\left(0.25e^{-\tau/4.4} + 0.75e^{-\tau/71}\right) \quad (2)$$

where τ is in msec. Thus, this suggests that of the 8.8×10^{19} ^{13}C nuclei on the NH_4-Y zeolite, 35% relax with an average T_1 of about 2.6 msec and 65% relax with an average T_1 of 82 msec. On the ultrastable H-Y zeolite, the 5.2×10^{19} ^{13}C nuclei detected are distributed as 25% which relax

with an average T_1 of 4.4 msec and 75% with an average T_1 of 71 msec. The centers of mass and the linewidths did not change significantly as τ was lengthened. However, the extremely weak signals for long τ values caused large experimental error limits, as much as 20 ppm for delays longer than 10 msec.

The lineshapes for two representative ^{13}C NMR spectra resulting from the 180^{o}-τ-90^{o} sequence for formic acid adsorbed on the NH_4-Y and the ultrastable H-Y zeolites at 295 K are shown in Figure 4. These lineshapes are for short delays, τ=0.5 msec, thus the two T_1 groups are overlapped in each spectrum. Although the linewidths are comparable to those of the reference formates, the spectral structures at the principal components of the chemical shift tensor are not as well resolved. The centers of mass of the ^{13}C lineshapes of the adsorbed formic acid are -164 ppm and -165 ppm, relative to TMS, for the NH_4-Y and the ultrastable H-Y substrates, respectively. This is within experimental error of pure formic acid: -163 ppm. Although these lines were fit with the same chemical shift regression analysis applied to the reference formates, the computed components are not as well defined and thus are rather ambiguous. The lineshape analysis data are reported in Table 2.

The quantitative data of the 180^{o}-τ-90^{o} experiment do not account for all of the ^{13}C originally deposited on the zeolites. The magnetization extrapolated to τ = 0 accounts for only 89% and 51% of the formic acid on the NH_4-Y and the ultrastable H-Y zeolites, respectively. A portion of the spins (less than about 3%) may be undetectable because the formate molecules are adsorbed within a critical radius of a paramagnetic impurity

(about 7 Å). The NMR signal from these species is extremely broad and would not be observed (35). The T_1 data and the spectra in Figure 4 were obtained after the zeolites had been loaded with the formic acid and stored at 273 K for four weeks. Figure 5 shows the spectra obtained for the ultrastable H-Y sample after an additional seven months at 273 K. The intensity of the broad line centered at -165 ppm has significantly decreased and there is a sharp feature at -180 ppm. This sharp line remains even when the proton decoupling is not applied, indicating that for this species, the coupling to the protons is less than its linewidth, 150 Hz. Since the isotropic chemical shift of pure CO is -181 ppm (34) and CO is the principal reaction product for formic acid on these zeolites, we attribute the sharp peak to physically adsorbed CO. Thus, at the time of the T_1 measurement, the formic acid had partially reacted to CO, which desorbed into the dead volume above the NMR sample, resulting in a reduced ^{13}C spin count.

2. Cross-polarization Experiments

The ^{13}C NMR signal intensity of the adsorbed formic acid as a function of the cross-polarization time is shown in Figure 6. The maximum magnetization for both zeolite samples was attained at approximately 0.6 msec. These data were also measured when the samples were four weeks old, the same time as the T_1 data in Figure 3. However, the signal from the ultrastable H-Y sample is greater than the signal from the NH_4-Y sample, although it was a factor of 1.7 less in the 180^0-τ-90^0 experiment. In general, the maximum obtainable signal enhancement for the ^{13}C-^1H cross-polarization is a factor of 4, provided that there is an infinite

proton spin bath relative to the ^{13}C spins and the ^{13}C and ^{1}H T_1's are long compared to the time constant of the heteronuclear interaction, T_{IS}. The ratios of the heat capacities of the ^{1}H and ^{13}C baths are 120:1 and 30:1 for the NH_4-Y and ultrastable H-Y zeolites, respectively, sufficient to approximate an infinite bath of ^{1}H spins. The maximum enhancements measured for the adsorbed formic acid are factors of 1.9 and 3.2 for the formic acid adsorbed on the NH_4-Y and ultrastable H-Y samples, respectively. Thus, the ultrastable H-Y sample has an effective ^{13}C-^{1}H magnetization transfer, but the NH_4-Y sample is considerably below the theoretical maximum.

The data in Figure 6 may be interpreted with the following thermodynamic model. The ^{13}C magnetization increases via transfer of magnetization from the ^{1}H spins. The rate of transfer is proportional to the difference in the spin-temperature between the two baths and is determined by the rate constant T_{IS}^{-1}. The ^{13}C magnetization decays by two processes: directly, by relaxation with the lattice, and indirectly, by transfer of magnetization back to the proton bath which, in turn, is directly relaxing with the lattice. Solving the coupled differential equations for the rate of change of the magnetization of the two spin systems and taking the limit of an infinite ^{1}H bath relative to the ^{13}C bath yields equation (3).

$$M_{xp}(t_{xp}) = \alpha_{xp} M_o \frac{\gamma_H}{\gamma_C} \left[\frac{T_{1C}T_{1H}}{T_{1C}T_{1H} + T_{IS}T_{1H} - T_{IS}T_{1C}} \right] \cdot \left[e^{-t_{xp}/T_{1H}} - \left(e^{-t_{xp}/T_{IS}} \right) \left(e^{-t_{xp}/T_{1C}} \right) \right] \quad (3)$$

Thus, the observed ^{13}C magnetization, M_{xp}, a function of the cross-polarization time, t_{xp}, grows exponentially with rate constant $(T_{IS}^{-1} + T_{1C}^{-1})$

and then decreases exponentially with rate constant T_{1H}^{-1}. The maximum enhancement of the magnetization relative to M_o is determined by the product of three prefactors: a term containing the three rate constants (which is about 1.0), the ratio of the gyromagnetic ratios γ_H/γ_C (which is 4.0), and an arbitrary normalization factor, α_{xp}. In general, α_{xp} is the fraction of the ^{13}C nuclei susceptable to the cross-polarization process before the magnetizations decay in the respective holding fields. The physical interpretation of the factor will be discussed later. T_{1C} and T_{1H}, the relaxation times in the respective holding fields, are determined experimentally. The data for formic acid on the NH_4-Y zeolite in Figure 6 are fit with T_{IS} = 0.23 msec, T_{1H} = 5.6 msec, and T_{1C} = 3.0 msec. The formic acid on the ultrastable H-Y sample is characterized by a shorter T_{IS}, 0.16 msec, indicating a stronger ^{13}C-^{1}H coupling, T_{1H} = 16 msec and T_{1C} = 5.0 msec. These values of T_{IS} are similar to those of the reference formates. The lines are relatively insensitive to the value of T_{1C}. The α_{xp} fractions are 0.52 and 0.83 for the NH_4-Y and ultrastable H-Y samples, respectively.

Typical spectra obtained by observing the proton-decoupled free-induction decays immediately after the ^{13}C holding pulses are shown in Figure 7. Although the signal-to-noise ratio is considerably better than that of the 180^o-τ-90^o experiment, the chemical shift components are again not resolved. Compared to the spectra from the 180^o-τ-90^o experiment, the lineshapes from the cross-polarization experiments are about 25% and 7% broader for the NH_4-Y and the ultrastable H-Y samples, respectively. The broader spectra are the result of the cross-polarization process emphasizing the signal from adsorbed species with broader lineshapes. In general, the

more stationary ^{13}C nuclei will have stronger ^{13}C-^{1}H couplings and thus will be enhanced more. The internuclear cross-polarization process for rapidly reorienting ^{13}C-^{1}H systems will be ineffective and these ^{13}C nuclei will be polarized only through ^{13}C-^{13}C homonuclear transfers or intramolecular ^{13}C-^{1}H couplings. Such processes would require about 5 to 10 msec of cross-polarization, as is necessary for the rapidly tumbling adamantane molecules at 295 K. For the adsorbed formic acid molecules, such long transfers are not possible since the magnetization in the holding fields decays before the process would be complete. Thus, the lineshapes in Figure 7 are primarily due to adsorbed formic acid molecules with nearly rigid ^{13}C-^{1}H bond systems.

The spectrum from the NH_4-Y sample broadens the most compared to the 180^{o}-τ-90^{o} spectrum, indicating that it contains a larger percentage of reorienting adsorbed species. The ultrastable H-Y sample has a much smaller change in linewidth. This is consistent with the enhancement factor of 3.2 which suggests that a larger percentage of the formic acid on the ultrastable H-Y sample is rigidly bonded to the substrate.

The center of mass frequencies of the cross-polarized spectra at 295 K are 17 and 15 ppm upfield from the 180^{o}-τ-90^{o} spectra for the NH_4-Y and the ultrastable H-Y zeolites, respectively. This also indicates that the cross-polarization technique is emphasizing a specific subgroup of the total lineshape. The isotropic frequencies on both samples at 295 K do not change as a function of the cross-polarization time for the range reported in Figure 6.

The cross-polarization spectra broaden and the isotropic frequencies move almost back to that of the 180^{o}-τ-90^{o} spectra as the temperature is

lowered, as seen in Figure 7. In addition, the general shapes of the spectra change, which is best visualized for the formic acid adsorbed on the NH_4-Y zeolite. The frequency at which the maximum intensity occurs shifts from the downfield side (i.e., the more negative side) of the isotropic frequency to the upfield side as the temperature is decreased. Spectra were measured at several intermediate temperatures, and it was observed that this shift is a gradual process. The lineshape parameters for the spectra in Figure 7 are given in Table 2.

The logarithm of the spectral area as a function of the delay from the end of the ^{13}C cross-polarization holding pulse to the echo for the formic acid adsorbed on the zeolites at 295 K is plotted in Figure 8. For each zeolite sample, the data decay with a single transverse relaxation time, T_2. The values of T_2 are 2.5 and 3.1 msec for the formic acid adsorbed on the NH_4-Y and the ultrastable H-Y zeolites, respectively. The center of mass frequencies and the linewidths of the spectra do not vary, within experimental limits, as a function of the echo time.

3. Dipolar-Modulation Experiments

The heteronuclear dipolar-modulation experiments were preformed on the formic acid adsorbed on the NH_4-Y zeolite at both 295 K and 125 K. The ^{13}C magnetization was first prepared by cross-polarization for 1.0 msec. Recall from previous results that the cross-polarization process will enhance selectively the more rigidly adsorbed formic acid molecules. The NMR signal was observed as an echo 1.2 msec after the end of the ^{13}C spin-locking pulse. Since the ^{13}C NMR spectra from the previous experiments do

not have well-resolved structure at the principal chemical shift components, it is not possible to assign the modulations in the lineshapes to distinct molecular orientations as was previously done with benzene and calcium formate (14,25). However, the variation of the spectral area as a function of the number of ^{1}H eight-pulse cycles (the dipolar-modulation time, see Figure 1) yields an average dipolar interaction and, thus, information on the average ^{13}C-^{1}H bond length and the extent of motional averaging (14). The spectral areas versus the dipolar-modulation time are shown in Figure 9. The spectral area of the adsorbed formic acid initially decreases at a rate comparable to that of calcium formate. Also note that the areas of the ^{13}C NMR spectra of calcium formate and benzene exhibit a damped oscillation about zero as predicted, but the spectral areas of adsorbed formic acid remain positive and do not oscillate.

4. Dipolar-Difference Experiment

The dehydration of formic acid requires necessarily the cleavage of the carbon-hydrogen bond. Thus, the ionic character of the carbonyl hydrogen attached to the adsorbed formate species, relative to formic acid, is of interest in the decomposition reaction. The average electron distribution of the hydrogen atom may be determined by measuring its chemical shift properties.

The linewidth of the homonuclear-decoupled ^{1}H NMR spectrum of the NH_4-Y zeolite at 295 K is about 26 ppm, as measured by the eight-pulse cycle. This broad Gaussian line is the sum of spectra from the hydrogens of the ammonium ions, the crystalline water, and the hydrogen bonded to the

carbon of the adsorbed formic acid. The dipolar-difference experiment eliminates the extraneous hydrogen signals and observes only the spectrum of the carbonyl hydrogen, approximately 3% of the total spectral intensity.

The ^{1}H NMR spectrum of the carbonyl hydrogen measured by the dipolar-difference experiment at 295 K for the formic acid adsorbed on the NH_4-Y zeolite is shown in Figure 10. It is similar to the ^{13}C NMR spectra in that it lacks any sharp structure but, in contrast, is much narrower, only 6.0 ppm wide at half-maximum intensity. The center of mass frequency for the spectrum is at about -12.3 ppm, relative to TMS. Though this experiment may not be calibrated a priori for an unknown system, the spectrum intensity indicates that the number of hydrogen species is on the order of the number of formate species.

IV. DISCUSSION

A. The Nature of the Adsorption of Formic Acid

A previous infrared study of the adsorption of formic acid on the NH_4-Y and ultrastable H-Y zeolites concluded that the acid was chemically adsorbed on the surfaces (1). Although the infrared spectra contained bands often attributed to physically adsorbed formic acid (36,37), there was no evidence of OH bending modes, and the adsorption isotherm indicated that the submonolayer was chemisorbed. The positions of the infrared bands were interpreted to be formic acid adsorbed as unidentate groups. As will be shown, the NMR data confirm that the formic acid is chemically adsorbed on both zeolites.

The ^{13}C NMR linewidths of the adsorbed formic acid are comparable to that of the solid reference formates. In general, the linewidth of the NMR spectrum of an adsorbed species may be the result of a number of interactions including paramagnetic broadening, heteronuclear dipolar broadening (from nuclei other than ^{1}H), spatial susceptibility inhomogeneities, and chemical shift anisotropy. These interactions have been discussed at length elsewhere (5,38). The dipolar interactions are the result of the molecular surroundings, such as the framework atoms of the zeolite supercage. The chemical shift broadening is an individual effect, determined by the electron distribution localized at the nucleus of interest.

Of the possible interactions, all but the chemical shift anisotropy can be eliminated by considering the ^{1}H spectrum of the carbonyl proton. If the other effects were the major causes of the ^{13}C NMR linewidth, the ^{1}H NMR spectrum would also be subjected to these effects and thus would be comparably broadened. However, the linewidth of the ^{1}H line is only 6 ppm, which places an approximate upper limit on the residual broadening of the ^{13}C NMR spectra.

Thus, the widths of the ^{13}C spectra are due primarily to chemical shift anisotropy. Such anisotropies are observed only in chemically adsorbed states. (However, there may still exist local motions at a site, as will be discussed later.) If a portion of the formic acid was physically adsorbed on the zeolite, the ^{13}C NMR line would contain an extremely narrowed component, as was observed for the CO decomposition product in Figure 5. Thus, all of the formic acid on the NH_4-Y and ultrastable H-Y zeolites is chemically adsorbed.

B. Spin-lattice Relaxation Times of Adsorbed Formic Acid

In many solids, particularly for ^{1}H spin systems, the homonuclear spin-spin coupling is much stronger than the spin-lattice coupling. Thus, the macroscopic magnetization decays uniformly and exponentially with time constant T_1. However, in dilute spin systems, the internuclear coupling is weak and each spin relaxes independently. For a homogeneous dilute system, the spins may still have a single T_1 since the spins are relaxing independently, but identically. However, if each spin should relax differently because of different local environments (e.g., paramagnetic impurities or nearby heteronuclear spins) or different motional properties, there would be a distribution of relaxation times in the sample. Such T_1 distributions are present in solid $C_6H_6CF_3$ because of an angular dependence of the heteronuclear coupling (39) and in CO on Rh on Al_2O_3 due to adsorption site heterogenity (8).

The ^{13}C T_1 data of the formic acid adsorbed on the zeolites may be interpreted by assuming that the formic acid has adsorbed in two states, each described by a different T_1. The relative proportions of the two states are given by the pre-exponential factors in equations (1) and (2). Both T_1's on either zeolite are extremely short and are typical of relaxation by a paramagnetic center. This is to be expected with the high Fe^{++} and Mn^{++} content of the samples. It is possible that the two T_1 groups represent chemically different formate species on the surface or that the T_1 distribution is the result of an inhomogeneous distribution of separations between the ^{13}C nuclei and the paramagnetic centers. The change in distributions between the short and long T_1's from the NH_4-Y to the

ultrastable H-Y samples (35:65 to 25:75) may be rationalized with either model. The infrared data suggest that the ultrastable H-Y zeolite contains a greater percentage of formate ions than the NH_4-Y sample (1). In this model, the longer T_1 group would be assigned to the formate ion and the shorter T_1 group to the unidentate structure. On the other hand, the transformation of the NH_4-Y zeolite to the ultrastable H-Y zeolite could have redistributed the paramagnetic centers and thus changed the distribution of T_1's.

The spectra from the T_1 experiment associated with the data points in Figure 3 did not change in width or isotropic frequency as τ was increased. However, the signal-to-noise ratios for the spectra with τ longer than about 10 msec became quite poor. Thus, if any subtle change in either quantity did occur, it would be difficult to detect. Recall that the isotropic chemical shifts for the entire range of formates do not vary more than about 8 ppm. Thus, although the T_1 data suggest a heterogeneity of surface states, it cannot be determined if the sites with different T_1's are chemically distinct.

C. Cross-polarization Experiments

The cross-polarization experiments also indicate that the formic acid is inhomogeneously adsorbed on the zeolites although in this case the basis for the differences may be unambiguously determined. The molecules are differentiated by the rate in which they cross-polarize, that is, by the strength of the dipolar coupling. The spectra shown in Figure 7(a) and 7(c), observed after 1.0 msec of cross-polarization at 295 K, contain primarily contributions from only those ^{13}C-^{1}H systems with semi-rigid

internuclear bonds. Those systems averaged by reorientations faster than the heteronuclear coupling (about 5 KHz) would require more than 5 msec to complete an intramolecular cross-polarization.

On the ultrastable H-Y zeolite, the intensity of cross-polarized ^{13}C NMR signal was a factor of 3.2 greater than the signal from the 180^{o}-τ-90^{o} experiment. The NH_4-Y sample was enhanced by only a factor of 1.9. These data may be interpreted by assuming that the surface contains two types of species: those that may be enhanced by the cross-polarization process by the theoretical maximum (a factor of 4) and those that are not cross-polarized in 1.0 msec. For the ultrastable H-Y sample, this assumption is probably realistic since the infrared spectrum of the adsorbed formic acid suggests that there are only two types of surface structures (1). However, the formic acid on the NH_4-Y zeolite exists in several different states, which probably have a distribution of heteronuclear dipolar couplings and thus the assumption is a more arbitrary distinction (1). With this assumption, the intensities of the cross-polarization spectra indicate that the distribution between the two groups is 52:48 on the NH_4-Y zeolite and 83:17 on the ultrastable H-Y zeolite. In order to interpret the two types of species, the chemical shift data must be considered.

D. The Relation of Chemical Shift Data to Formate Structures

The formate group bonds in a range of configurations from the ester-like unidentate compounds (species I) covalently bonded through a single oxygen atom, to the bidentate structure where the formate ion is chelated about one or more metal ions (species II and III). The structural parameters of a few compounds are listed in Table 1B. One index of the

bonding of the formate group is the ratio of the two carbon-oxygen bond lengths. This ratio ranges from 1.12 for methyl formate to about 1.00 for calcium formate.

The chemical shift information for these formate compounds is presented in Table 1A. The isotropic chemical shifts of the compounds, $\tilde{\sigma}$, does not correlate with the geometry of the formate group. This was first observed by Ackerman, et al. in a study of the two crystallographically distinct forms of calcium formate (16). The overall anisotropy, $\sigma_{33} - \sigma_{11}$, tends to decrease as R_2/R_1 decreases, but the scatter in the correlation is extremely large. There is, however, a very good correlation between the position of the central principal component, σ_{22}, and the ratio of the carbon-oxygen bond lengths. As the bond lengths become more symmetric, σ_{22} moves from the upfield side of the powder pattern to the downfield side. This is reflected in the ratio of the difference between the upfield component and the central component, $\sigma_{22} - \sigma_{11}$, to the overall anisotropy, $\sigma_{33} - \sigma_{11}$. This ratio ranges from 0.20 for methyl formate ($R_2/R_1 = 1.12$) to 0.66 for calcium formate ($R_2/R_1 = 1.00$). Thus, in general, for bidentate formate ions $(\sigma_{22} - \sigma_{11})/(\sigma_{33} - \sigma_{11})$ is on the order of 0.6, and for ester-like formate groups the ratio is closer to 0.3. As this correlation is based on relatively few data points, the relation between these two parameters does not permit a reliable calculation of the R_2/R_1 from the chemical shift components, only the general trend.

E. The Molecular Structure of the Adsorbed Formic Acid

The relation between the ^{13}C chemical shift components and the

symmetry of the formate group may be used to determine the state of the adsorbed formic acid. The chemical shift components are meaningful only in ^{13}C powder patterns without appreciable motional averaging. The spectra from the 180^{o}-τ-90^{o} experiment at 295 K, which contain motionally averaged contributions, are not applicable. However, the cross-polarization experiment observes selectively the more rigid species for short cross-polarization times, i.e., about 1.0 msec. Thus, the rigid components of the 180^{o}-τ-90^{o} spectra at 295 K in Figure 4, isolated by the cross-polarization technique, are shown in Figure 7. The values of the ratio $(\sigma_{22} - \sigma_{11})/(\sigma_{33} - \sigma_{11})$ for the cross-polarized spectra at 295 K for the formic acid adsorbed on the NH_4-Y and ultrastable H-Y zeolites are 0.69 and 0.58, respectively. These relatively high values of this ratio argue that this species is a semi-rigidly bonded formate ion, with approximately symmetric carbon-oxygen bond lengths. Furthermore, the degree of enhancement of the cross-polarization technique, discussed earlier, indicates that the formate ion species comprises 52% and 83% of the formic acid adsorbed on the NH_4-Y and ultrastable H-Y zeolites, respectively.

When the cross-polarization experiment is repeated at reduced temperatures, the central component of the powder patterns shifts from the downfield side to the upfield side, as mentioned earlier. Thus, the ratio $(\sigma_{22} - \sigma_{11})/(\sigma_{33} - \sigma_{11})$ changes from 0.69 to 0.41 on the NH_4-Y sample and from 0.58 to 0.33 on the ultrastable H-Y sample. These transitions may be attributed in part to a quenching of the motions responsible for the averaging of the other species at room temperature. If the motionally averaged group had a $(\sigma_{22} - \sigma_{11})/(\sigma_{33} - \sigma_{11})$ ratio on the order of the

unidentate formate groups, about 0.20, the incorporation of this species into the powder pattern would lower the average ratio. However, on both samples the added contributions from this species do not account for the large decreases in the ratios. For example, if 83% of the formic acid on the ultrastable H-Y zeolite is adsorbed as formate ions, the contribution from the remaining 17% is not sufficient to cause $(\sigma_{22} - \sigma_{11})/(\sigma_{33} - \sigma_{11})$ to decrease from 0.58 to 0.33. One interpretation of the large change is that upon cooling to temperatures below 150 K, some of the surface formate structures convert from ionicly bound bidentate groups to unidentate structures. This interpretation is supported by the fact that upon cooling, the isotropic chemical shift does not return to the value measured by the 180^{o}-τ-90^{o} experiment. However, because of the lack of pronounced features in the powder patterns, the fitted chemical shift components may be somewhat arbitrary, that is, changing any of the components by 10% will not cause a large change in the error of the fitted spectrum. Thus, there may be errors as great as 10% in the computed ratios and the incorporation of the unidentate species may actually be sufficient to explain the shifts.

Regardless of the exact ratios, there is a definite change in the symmetries of the cross-polarization spectra upon cooling from 295 K to below 150 K. This transition is probably due to the addition of the unidentate groups which have become more rigid at the lower temperatures. There may also be some conversion of bidentate ions to unidentate groups although this interpretation will require further study.

The assignment of the cross-polarization data to unidentate and bidentate structures on the surface is in agreement with the results of an infrared study (1). The approximate distributions between the two groups (52:48 on the NH_4-Y zeolite and 83:17 on the ultrastable H-Y zeolite) also agree with the qualitative distributions based on the relative intensities of the infrared spectra peaks.

F. The Nature of the Bidentate Formate Ion Surface Species

As discussed in the Introduction, the ultrastable H-Y zeolite is catalytically more active than the NH_4-Y zeolite. The infrared spectra and the NMR data indicate that there is an increased percentage of the formate ions on the ultrastable H-Y surface. Thus, if the direct decomposition of the formate ion is the rate-determining step in the dehydration reaction to CO and H_2O (2), the structure of the adsorbed state is of interest. By isolating the ^{13}C NMR signal of the formate ion with the cross-polarization process at 295 K, it is possible to determine the adsorption site, the ^{13}C-^{1}H bond characteristics, and the ionic character of the carbonyl hydrogen.

In the presence of proton-decoupling, the main sources of broadening of the ^{13}C NMR spectra are chemical inhomogeneity of the species, librational motion, lifetime broadening, and dipolar broadening from the ^{27}Al. The full widths at half-maximum of the Gaussian broadening functions convoluted with the chemical shift powder pattern of the cross-polarization spectra at 295 K, spectra 7(a) and 7(b), are 124 and 142 ppm for the NH_4-Y and ultrastable H-Y samples, respectively. The second moments for these broadening functions are 0.67 G^2 and 0.88 G^2, respectively. The

contributions due to chemical inhomogeneities and librational motions are estimated from the broadening in the reference formates, which is about 0.08 G^2. The lifetime broadenings, computed from the T_2's, are 0.14 G^2 for the NH_4-Y and 0.09 G^2 for the ultrastable H-Y samples. The remainder of the broadening is attributed to the ^{13}C-^{27}Al dipolar interaction. The second moment of this interaction may be calculated from the Van Vleck equation for heteronuclear broadening shown below (40).

$$\langle \Delta^2\omega \rangle_{IS} = \frac{1}{3} \gamma_S^2 \hbar^2 s(s+1) \frac{1}{N} \sum_{j,k} \frac{(1 - 3\cos^2 \theta_{jk})}{r_{jk}^6} \qquad (4)$$

In equation 4, the second moment of the ^{13}C spectrum due to ^{27}Al is determined by the gyromagnetic ratio of ^{27}Al, 6.97 x 10^3 rad G^{-1} sec^{-1}; $\hbar$, 1.05 x 10^{-3} $G^2\text{Å}^3$ sec; the spin of the ^{27}Al nucleus, S = 5/2, and the ^{13}C-^{27}Al internuclear vector of length r at an angle θ with the external magnetic field. The sum is over all ^{13}C and ^{27}Al spins in the sample, normalized by N, the number of ^{13}C spins. For a polycrystalline sample, the spherical average of the angular dependence is 4/5. For a formate ion bonded to an Al ion, the bidentate would be similar to the Na, Ca, and Sr salts, and the ^{13}C-^{27}Al internuclear distance is 2.75 Å. With this configuration, equation 4 yields a second moment of 0.29 G^2. The contribution from Al atoms in the surrounding zeolite framework, not directly bonded to the formate ion, is estimated to be about 0.15 G^2. Thus, the ^{13}C-^{27}Al broadening is calculated to be 0.44 G^2 for a formate ion directly bonded to the Al atom and 0.15 G^2 when bonded to a Si atom.

However, this interaction will increase if the ^{27}Al nuclei are in a non-

Zeeman state; that is, it is possible that large electrostatic field gradients at the zeolite surface determine the orientation of the quadrupolar ^{27}Al rather than the external magnetic field. It has been observed that for amorphous aluminas, the ^{27}Al $1/2 \longleftrightarrow -1/2$ transition vanishes in samples with BET surface areas greater than about 100 m^2g^{-1}, indicating that the ^{27}Al nuclear alignment is determined by local electrostatic fields (41). In the case of spin 1/2 - spin 7/2 systems if the spin 7/2 is in a non-Zeeman state, the second moment may increase by as much as a factor of 1.8 (42). Similarly, it has been shown that the non-Zeeman state of ^{27}Al (spin 5/2) may also result in as much as a factor of 1.8 increase in the second moment of the ^{13}C lineshape (43). Thus, the total second moment, including the librational contribution, is about 0.52 to 0.87 G^2 for the formate ion bonded directly to the Al atom and about 0.23 to 0.35 G^2 for the formate ion bonded to a Si atom. The second moments of the observed broadenings of the chemical shift powder patterns, minus the lifetime contributions are 0.53 G^2 for the NH_4-Y sample and 0.79 G^2 for the ultra-stable H-Y sample. Thus, the residual dipolar broadening indicates that the formate ion is bonded to the Al ions.

The dipolar-modulation data for the formate ion in the NH_4-Y zeolite, shown in Figure 9, indicate that the ^{13}C-^1H coupling is similar to that of calcium formate. The initial decrease of the spectral area for both calcium formate and the surface formate ion is less than predicted for a bond length of 1.09 Å, shown by the dotted line in Figure 9. The bond length in calcium formate measured by X-ray diffraction is 1.09 Å. The slower decrease in the oscillation of the spectral area compared to the

theoretical rate has been attributed to librational motions in the calcium formate (14,25). We propose that the adsorbed formate ion internuclear bond length is also 1.09 Å and is undergoing motions similar to those in calcium formate. Also, as the dipolar-modulation time is increased, the area of the adsorbed formic acid spectra do not decrease below zero, contrary to the data of calcium formate and solid benzene. It is suggested that although the direct ^{1}H-^{1}H coupling is suppressed by the eight-pulse cycles, the ^{1}H nuclei are still coupled through the ^{27}Al nuclei. Thus, after about 0.1 msec, the ^{1}H-^{27}Al-^{1}H spin diffusion has destroyed some of the phase coherence in the expeirment.

The dipolar-difference experiment selectively observes the ^{1}H bonded to the ^{13}C nuclei where the internuclear bond is rigid. Thus, the ^{1}H spectrum in Figure 10 is the carbonyl proton of the formate ion on the NH_4-Y zeolite at 295 K. As was discussed earlier, the ionic character of this proton is of importance to dehydration reaction mechamisms. The isotropic chemical shift of this spectrum, -12.3 ppm relative to TMS, is similar to that of formate salts. It has been reported previously that the equivalent protons in calcium formate and ammonium formate have isotropic chemical shifts of -10.9 ppm and -12.8 ppm, whereas formic acid is further upfield, at -9.2 ppm (15). The downfield shift of the chemical shift of the carbonyl hydrogen suggests that the hydrogen has acquired a more acidic nature. Thus, the hydrogen may be more susceptible to nucleophilic attack, or it may more readily shift to electron-rich centers.

V. CONCLUSIONS

The results of solid state NMR experiments have determined that formic acid is chemically adsorbed on the NH_4-Y and ultrastable H-Y zeolites in two states, differentiated by the strength of the ^{13}C-^{1}H dipolar coupling. The difference in heteronuclear couplings is attributed to differences in motional properties. Based on the symmetry of the chemical shift tensors, the more rigidly adsorbed state is interpreted to be a bidentate formate ion. The other surface species becomes rigid at temperatures below 150 K. Changes in the chemical shift tensor upon cooling indicate that this other species is a unidentate formate group. From the enhancements obtained by the cross-polarization technique, relative to the 180^{o}-τ-90^{o} *experiment*, it is determined that the ratio of bidentate to unidentate groups is 52:48 on the NH_4-Y zeolite and 83:17 on the ultrastable H-Y zeolite. These values are for loadings of about 0.3 monolayer on both the NH_4-Y and ultrastable H-Y zeolites. These results are in agreement with the qualitative interpretations of a previous infrared study of similar loadings of formic acid on the two zeolites (1).

The ^{13}C NMR spectrum of the formate ion may be selectively observed by the cross-polarization technique at 295 K. The magnitude of the broadening in the spectrum that is attributed to ^{27}Al dipolar interactions indicates that on both zeolites, the formate ion is bonded to Al atoms in the zeolite supercages. The initial behavior of the dipolar-modulation data for the adsorbed formate ion are similar to that of calcium formate. These data are interpreted as a ^{13}C-^{1}H bond of 1.09 $\mathring{A}$ in a librational

motion comparable to that of calcium formate. The isotropic chemical shift of the carbonyl hydrogen of the surface formate ion is similar to those of other bidentate salts, rather than formic acid. The more acidic nature of this hydrogen may be involved in the cleavage of the carbon-hydrogen bond. The center of mass of the bidentate formate ion is much lower than other formate salts, by at least 15 ppm. Though this may have implications in the state of the ion, the complex combination of paramagnetic and diamagnetic contributions does not allow an interpretation of the ionic state of the carbon atom.

The motional averaging of the unidentate is most likely a reorientation at the adsorption site, such as rotation about the zeolite-oxygen bond or the carbon-oxygen bond. It is conceivable that the different bonding to the zeolite surface is the result of formic acid bonding to Si atoms.

The distribution of adsorbed states of formic acid on the two zeolites suggests that the ultrastable H-Y zeolite has more Al sites available for adsorption. In addition, the ^{13}C-^{27}Al dipolar interaction of the formate ions on the ultrastable H-Y zeolite is stronger as evidenced by the second moments of the broadenings, 0.79 G^2 compared to 0.53 G^2. The increased number of Al atoms with stronger couplings to formate groups is consistent with the proposal that the thermal decomposition of NH_4-Y to ultrastable H-Y creates 9 to 15 nonframework Al ions in the zeolite supercages (17).

VI. ACKNOWLEDGEMENTS

This work was supported in part by the Office of Naval Research, under contract N00014-75-0960. The authors wish to thank J. A. Reimer for obtaining the dipolar-modulation and dipolar-difference spectra, G. W. Brudvig for measuring the electron paramagnetic spectra of the zeolites, and Dr. G.T. Kerr of Mobil Oil Research and Development for supplying the zeolite samples. We also are indebted to Professor S. I. Chan for helpful discussions and comments.

References

1. T. M. Duncan and R. W. Vaughan, J. Catalysis, submitted.
2. J. J. F. Scholten, P. Mars, P. G. Menon, and R. Van Hardeveld, Proc. Intern. Cong. Catalysis, 3rd, Amsterdam, 1964, p. 881.
3. E. G. Derouane, J. Fraissard, J. J. Fripiat and W. E. E. Stone, Catalysis Reviews 7, 121 (1972).
4. H. Pfeifer, Nuclear Magnetic Resonance, Vol. 7, P. Diehl, E. Fluck and R. Kosfeld, Eds., (Springer-Verlag, New York, 1972), p. 55.
5. K. J. Packer, Progr. NMR Spectroscopy 3, 81 (1967).
6. S. Kaplan, H. A. Resing and J. S. Waugh, J. Chem. Phys. 59, 5681 (1973).
7. E. O. Stejskal, J. Schaefer, J. M. S. Henis and M. K. Tripoli, J. Chem. Phys. 61, 2351 (1974).
8. T. M. Duncan, J. T. Yates, Jr., and R. W. Vaughan, J. Chem. Phys., Submitted
9. R. W. Vaughan, Ann.Rev. Phys. Chem. 29, 397 (1978).
10. M. Mehring, High Resolution NMR Spectroscopy in Solids, (Springer-Verlag, New York, 1976).
11. U. Haeberlin, High Resolution NMR in Solids - Selective Averaging, (Academic Press, New York, 1976).
12. (a) A. Pines, M. G. Gibby and J. S. Waugh, J. Chem. Phys. 56, 1776 (1972);
    (b) A. Pines, M. G. Gibby, and J. S. Waugh, J. Chem. Phys. 59, 569 (1973).
13. D. E. Demco, J. Tegenfeldt, and J. S. Waugh, Phys. Rev. B 11,

4133 (1975).

14. (a) M. E. Stoll, A. J. Vega and R. W. Vaughan, J. Chem. Phys. 65, 4093 (1976);

(b) M. E. Stoll, A. J. Vega and R. W. Vaughan, XIXth Congress Ampere, Heidelberg, 1976.

15. J. A. Reimer and R. W. Vaughan, Chem. Phys. Lett. 63, 163 (1979).

16. J. L. Ackerman, J. Tegenfeldt, and J. S. Waugh, J. Amer. Chem. Soc. 96, 6843 (1974).

17. (a) G. T. Kerr, J. Catalysis 15, 200 (1969); (b) G. T. Kerr, Adv. in Chem. Series 121, 219 (1973); (c) C. V. McDaniel and P. K. Maher, Molecular Sieves, (Soc. Chem. Industry, London, 1967) p. 186.

18. S. A. Al'tshuler and B. M. Kozyrev, Electron Paramagnetic Resonance in Compounds of Transition Elements, 2nd ed., Eng. Trans. from Russian, (Wiley, New York, 1974).

19. A. S. Coolidge, J. Amer. Chem. Soc. 50, 2166 (1928).

20. C. V. McDaniel and P. K. Maher, Zeolite Chemistry and Catalysis, J. A. Rabo, ed., ACS Monograph 171, Washington, D. C., 1976, p. 296.

21. R. W. Vaughan, D. D. Elleman, L. M. Stacey, W. K. Rhim, and J. W. Lee, Rev. Sci. Inst. 43, 1356 (1972).

22. M. E. Stoll, A. J. Vega and R. W. Vaughan, Rev. Sci. Inst. 48, 800 (1977).

23. (a) H. Y. Carr and E. M. Purcell, Phys. Rev. 94, 630 (1954);

(b) R. L. Vold, J. S. Waugh, M. P. Klein, and D. E. Phelps, J. Chem. Phys. 48, 3831 (1968).

24. S. R. Hartmann and E. L. Hahn, Phys. Rev. 128, 2042 (1962).

25. M. E. Stoll, Ph.D. Thesis, Caltech, 1977.

26. W-K. Rhim, D. D. Elleman, L. B. Schreiber and R. W. Vaughan, J. Chem. Phys. 60, 1595 (1974).

27. M. Mehring, A. Pines, W-K. Rhim and J. S. Waugh, J. Chem. Phys. 54, 3239 (1971).

28. N. Bloembergen and J. A. Rowland, Acta Metall. 1, 731 (1953).

29. A. Pines, M. G. Gibby, J. S. Waugh, Chem. Phys. Lett. 15, 373 (1972).

30. J. M. O'Gorman, W. Shand, Jr., and V. Schomaker, J. Amer. Chem. Soc. 72, 4222 (1950).

31. R. G. Lerner, B. P. Dailey, and J. P. Friend, J. Chem. Phys. 26, 680 (1957).

32. I. Nahringbauer, Acta. Cryst. B 24, 565 (1968).

33. I. Nitta and K. Osaki, X-Rays 5, 37 (1948); ref. in Structural Reports 11, 556 (1948).

34. J. B. Stothers, Carbon-13 NMR Spectroscopy, (Academic Press, New York, 1972).

35. A. Abragam, The Principles of Nuclear Magnetism, (Oxford University Press, London, 1961), Chap. IX

36. A. Bielanski and J. Datka, J. Catalysis 32, 183 (1974).

37. K. Hirota, K. Fueki, K. Shindo and Y. Nakai, Bull. Chem. Soc. Japan, 32, 1261 (1959).

38. M. D. Sefcik, J. Schaeffer and E. O. Stejskal, Molecular Sieves-II, J. R. Katzer, ed. ACS Symposium Series 40, Washington, D. C. 1977,

p. 344.

39. J. E. Anderson and W. P. Slichter, J. Chem. Phys. 43, 433 (1965).

40. Reference 35, Chapter IV.

41. (a) D. E. O'Reilly, J. Chem. Phys. 28, 1263 (1958); (b) D. E. O'Reilly, Adv. in Catalysis 12, 31 (1960).

42. D. L. Vanderhart, H. S. Gutowsky, T. C. Farrar, J. Amer. Chem. Soc. 89, 5056 (1967).

43. D. L. Vanderhart, private communication.

TABLE 1

Reference Formates

A. ^{13}Chemical Shift Parameters

Compound	Temperature (K)	Principal Components[a] σ_{11}	σ_{22}	σ_{33}	$\tilde{\sigma}$	$\sigma_{33}-\sigma_{11}$	$\frac{\sigma_{22}-\sigma_{11}}{\sigma_{33}-\sigma_{11}}$	Reference
$HCOOCH_3$[b]	87	-107	-136	-253	-165	146	0.20	29
HCOOH[c]	125	-92	-162	-252	-169	160	0.44	This Work
$(NH_4)HCO_2$	185	-99	-168	-225	-164	126	0.55	This Work
$Ca(HCO_2)_2$	125	-96	-186	-235	-172	139	0.66	This Work

B. Structure

Compound	C-O Bond Lengths (Å) R_1	R_2	R_2/R_1	Method	Reference
$HCOOCH_3$	1.22 ± 0.03	1.37 ±0.04	1.12	electron diffraction	30
HCOOH	1.245 ± 0.002	1.312 ± 0.002	1.05	isotopic microwave	31
$(NH_4)HCO_2$	1.237 ± 0.007	1.246 ± 0.007	1.01	X-ray diffraction	32
$Ca(HCO_2)_2$[d]	1.25 ± 0.03 1.24 ± 0.03	1.25 ± 0.03 1.25 ± 0.03	1.00 1.01	X-ray diffraction	33

(a) in ppm, relative to tetramethylsilane (TMS)

(b) data converted from original reference using $\sigma(C_6H_6)$ = -128.7 ppm, relative to TMS

(c) principal components estimated from data, rather than computed lineshape.

(d) two crystallographically distinct formate groups.

TABLE 2

^{13}C Spectral Parameters of Adsorbed Formic Acid

A. HCOOH on the NH_4-Y Zeolite

Spectrum	Experiment	Temperature (K)	Linewidth[a]	Principal Components[b] σ_{11}	σ_{22}	σ_{33}	$\tilde{\sigma}$	$\frac{\sigma_{22}-\sigma_{11}}{\sigma_{33}-\sigma_{11}}$	δ
4(a)	180^0-τ-90^0	295	60	-153	-168	-172	-164	0.79	103[e]
7(a)	Cross-Polarization	295	75	-129	-151	-161	-147	0.69	124
7(b)	Cross-Polarization	150	111	-95	-152	-233	-160	0.41	53

B. HCOOH on the Ultrastable H-Y Zeolite

4(b)	180^0-τ-90^0	295	98	-112	-176	-206	-165	0.68	100[e]
7(c)	Cross-Polarization	295	105	-95	-155	-199	-150	0.58	142
7(d)	Cross-Polarization	115	144	-98	-145	-240	-161	0.33	116

(a) Full width at half-maximum, in ppm

(b) in ppm, relative to TMS

(c) Isotropic frequency of the lineshape, relative to TMS

(d) Linewidth of the Gaussian broadening function convoluted into the powder pattern, in ppm

(e) Spectrum convoluted with a Lorentzian broadening function

FIGURE CAPTIONS

Figure 1. Schematic representations of the NMR pulse schemes used in this study. The abscissa for these representations is time and the pulses are indicated by rectangular boxes of arbitrary height. The observed magnetization is indicated by the dotted lines. The ^{13}C and ^{1}H pulse schemes are started simultaneously. In the 180^{o}-τ-90^{o} and dipolar-difference sequences, the ^{13}C A and B modes are alternately applied and the NMR signal is alternately added and subtracted.

Figure 2. ^{13}C NMR spectra of reference formates measured by ^{13}C-^{1}H cross-polarization. (a) Formic acid at 125 K, (b) ammonium formate at 185 K and (c) calcium formate at 125 K. The abscissa scale is 3.44 ppm per point in all spectra. Frequencies are relative to tetramethylsilane (TMS).

Figure 3. Amplitude of the observed ^{13}C magnetization versus τ, the delay between the 180^{o} and 90^{o} pulses, for formic acid adsorbed on the NH_4-Y (□) and the ultrastable H-Y (Δ) zeolites at 295 K. Absolute counts for the ^{13}C nuclei were calibrated with an enriched adamantane sample. The proton-decoupling was set at 16 G.

Figure 4. ^{13}C NMR spectra of formic acid adsorbed on (a) the NH_4-Y zeolite (130,000 averages) and (b) the ultrastable H-Y zeolite (66,000 averages), as measured by the 180^{o}-τ-90^{o} experiment at 295 K. In both spectra, τ = 0.5 msec and

proton decoupling was at 16 G.

Figure 5. ^{13}C NMR spectra of the ultrastable H-Y zeolite dosed with formic acid, eight months later, with (a) 16 G proton decoupling and (b) no decoupling. Both spectra are the result of about 66,000 averages of the 180^{o}-τ-90^{o} sequence with τ = 0.5 msec at 295 K.

Figure 6. The amplitude of the observed ^{13}C magnetization versus the length of the cross-polarization process for formic acid adsorbed on the NH_4-Y (□) and the ultrastable H-Y (△) zeolites at 295 K. The proton decoupling was set at 16 G.

Figure 7. ^{13}C NMR spectra of adsorbed formic acid as a function of temperature, measured by the cross-polarization scheme. The data were recorded immediately after 1.0 msec of cross-polarization with 16 G of proton decoupling. The spectra are formic acid adsorbed on the NH_4-Y zeolite at (a) 295 K and at 155 K; and the ultrastable H-Y zeolite at (c) 295 K and at 115 K. Each spectrum is the accumulation of about 66,000 averages.

Figure 8. The amplitude of the observed ^{13}C magnetization versus the delay to the echo in the cross-polarization sequence for formic acid adsorbed on the NH_4-Y zeolite (□) and the ultra-stable H-Y zeolite (△) at 295 K. Proton decoupling pulses of 16 G were applied immediately after the ^{13}C spin-locking pulses.

Figure 9. Spectral areas versus the dipolar-modulation time for formic acid adsorbed on the NH_4-Y zeolite at 295 K (□) and at 125 K (△). For comparison, we also plot the data for benzene at 185 K (◇) and calcium formate at 295 K (○) reported by Stoll, et al. (14,25). Theoretical curves are for a rigid ^{13}C-^{1}H bond length of 1.09 Å (dotted line), a rigid bond at 1.19 Å (dashed line), and for a 1.09 Å bond averaged by rotation in a plane (dashes and dots).

Figure 10. Proton spectrum of the carbonyl hydrogen of formic acid adsorbed on the NH_4-Y zeolite at 295 K, obtained with about 8,000 averages of the dipolar-difference experiment.

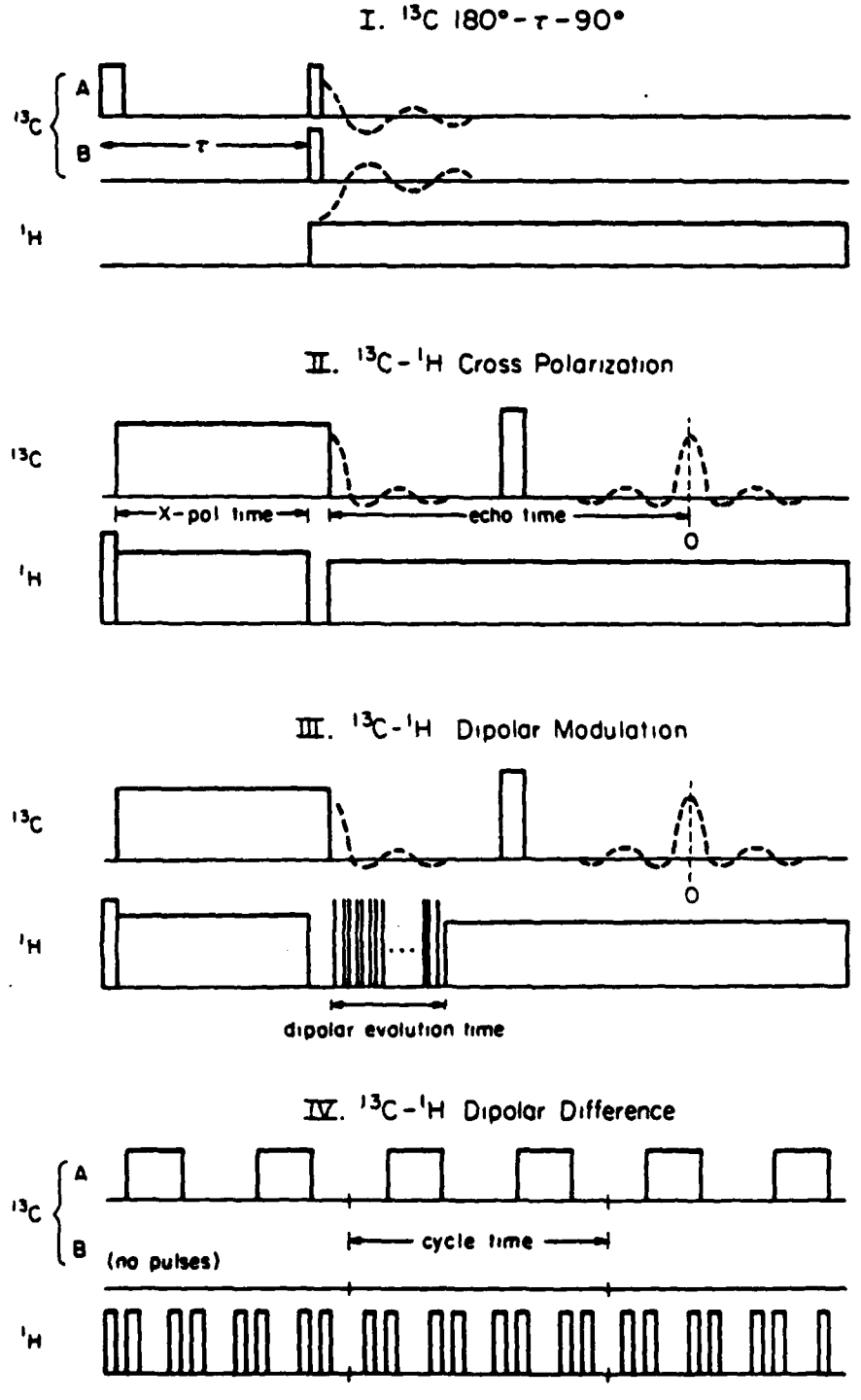
I. ^{13}C 180°-τ-90°
^{13}C
A
B
τ
^{1}H
II. ^{13}C-^{1}H Cross Polarization
^{13}C
X-pol time
echo time
O
^{1}H
III. ^{13}C-^{1}H Dipolar Modulation
^{13}C
O
^{1}H
dipolar evolution time
IV. ^{13}C-^{1}H Dipolar Difference
^{13}C
A
B
cycle time
(no pulses)
^{1}H

Figure 1.

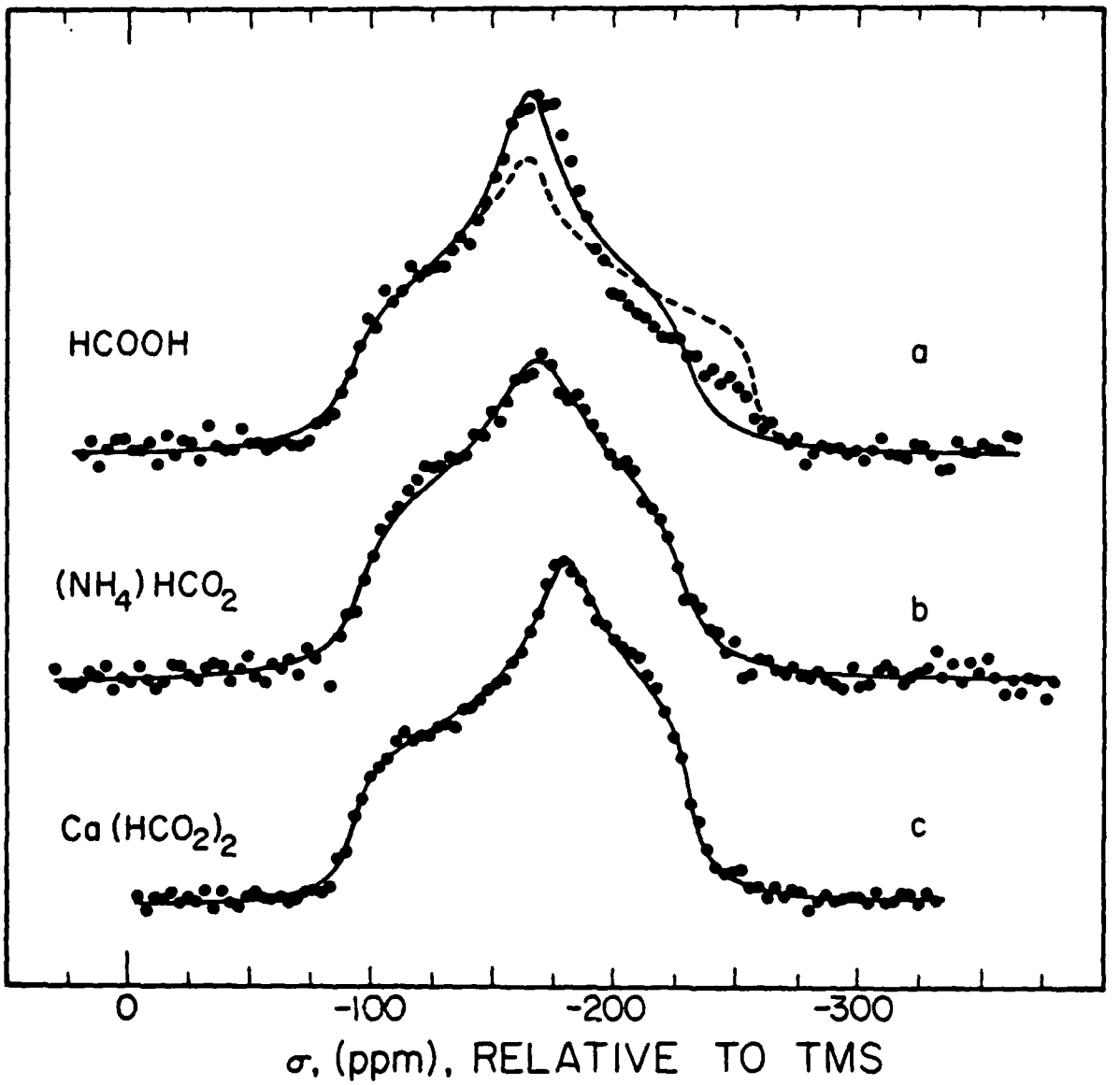

Figure 2.

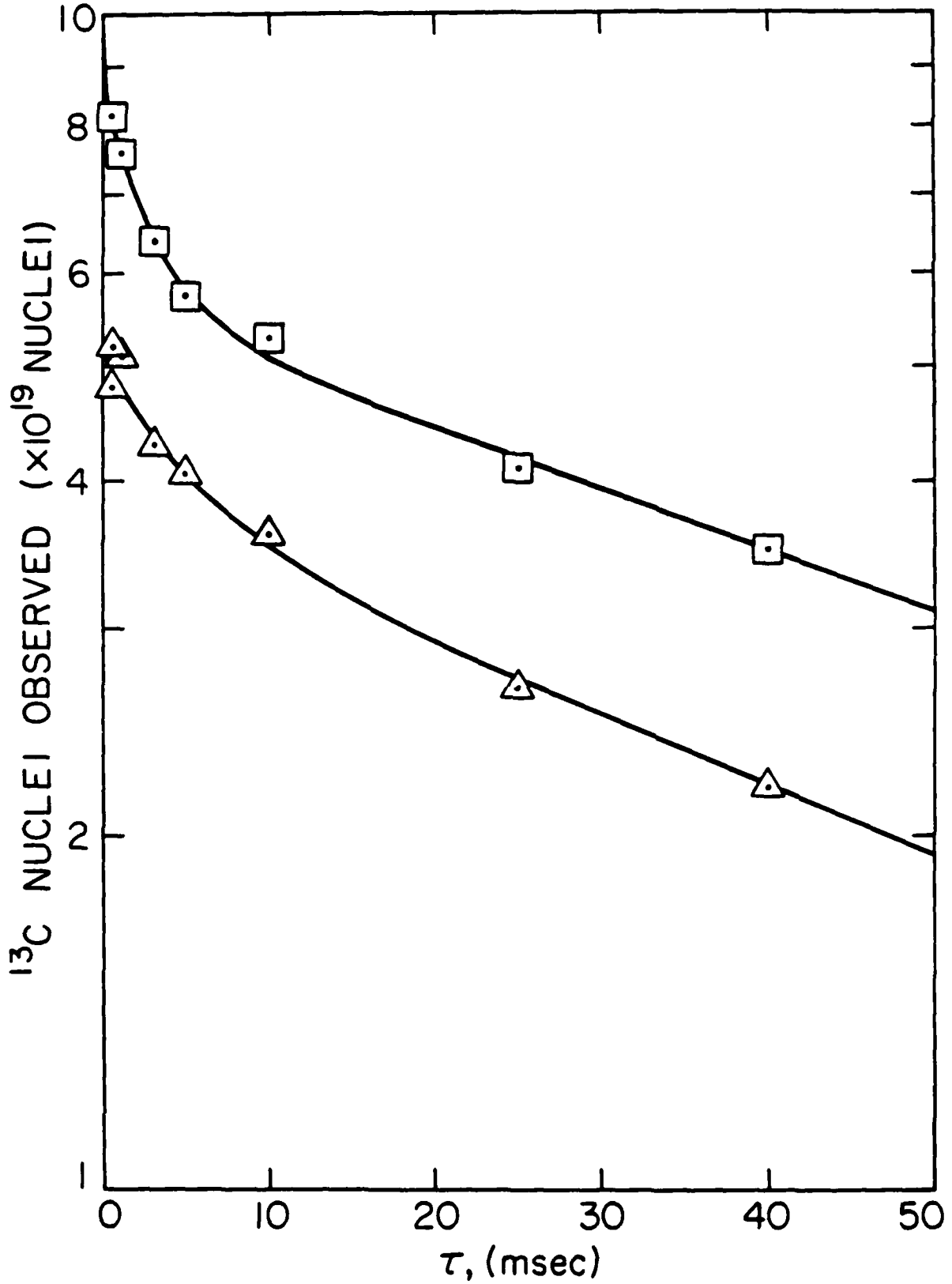
10
8
6
4
2
1
0
10
20
30
40
50
^{13}C NUCLEI OBSERVED ($\times 10^{19}$ NUCLEI)
τ, (msec)

Figure 3.

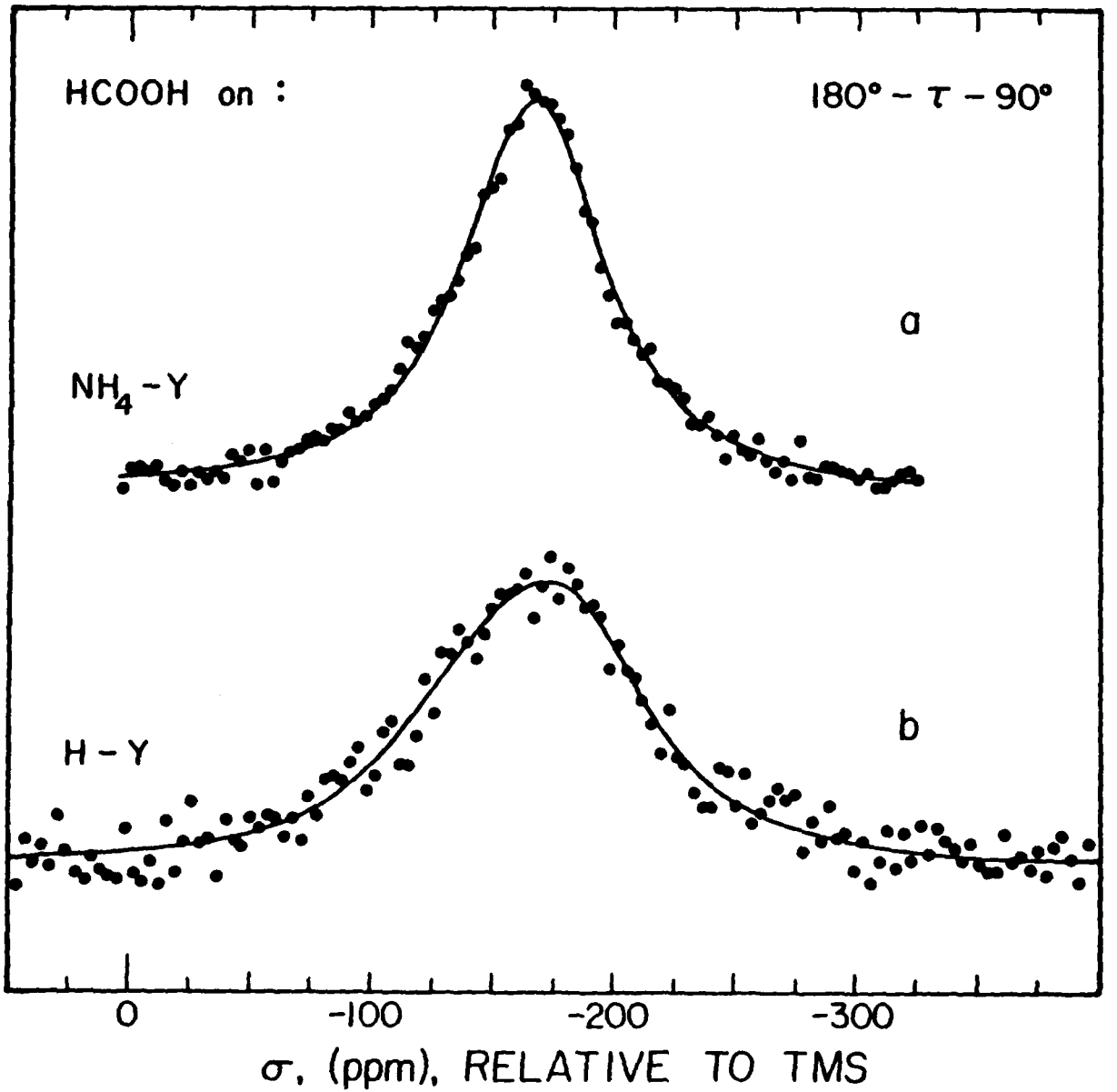

Figure 4.

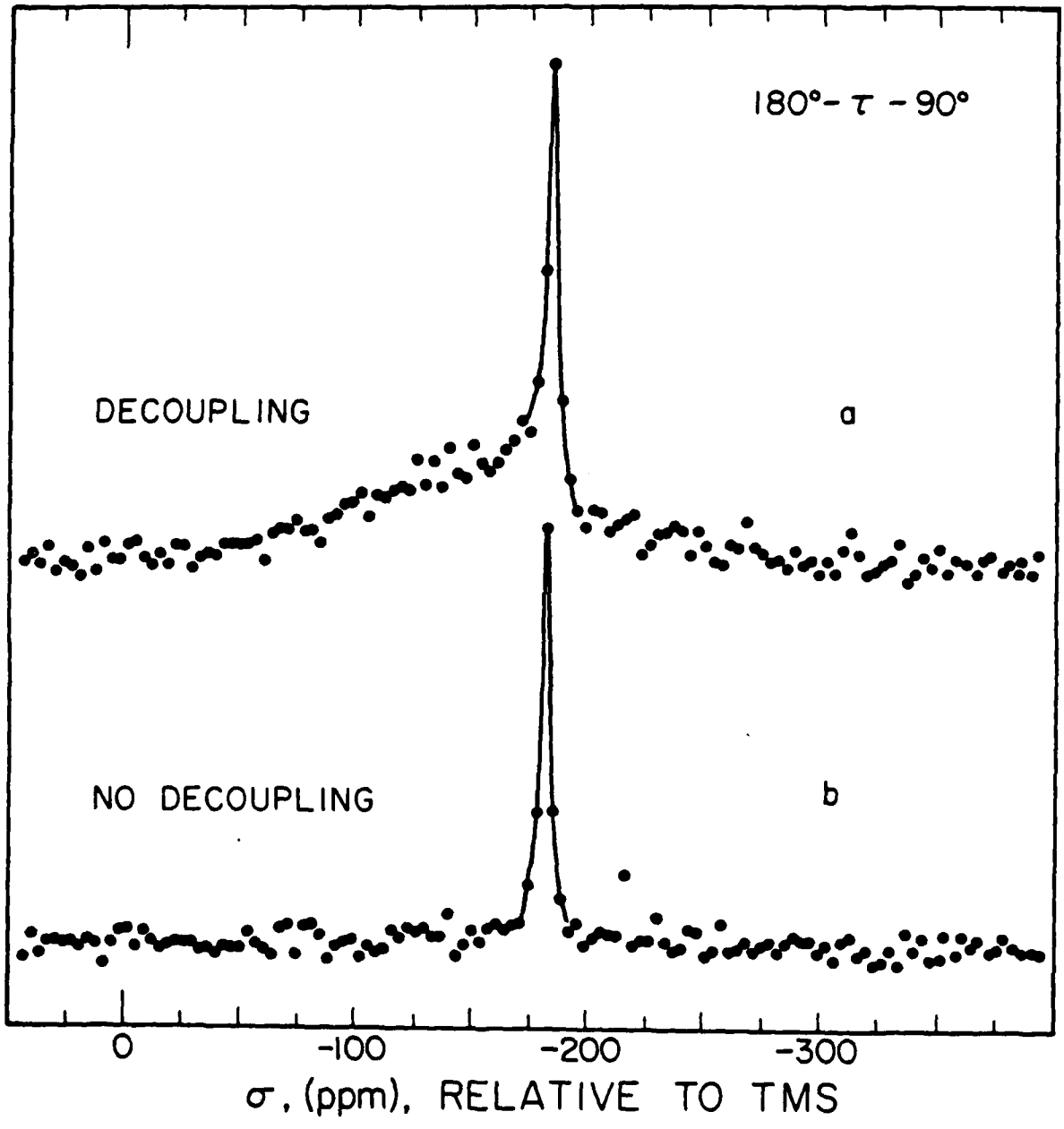
180°- τ - 90°
DECOUPLING
a
NO DECOUPLING
b
0
-100
-200
-300
σ, (ppm), RELATIVE TO TMS

Figure 5

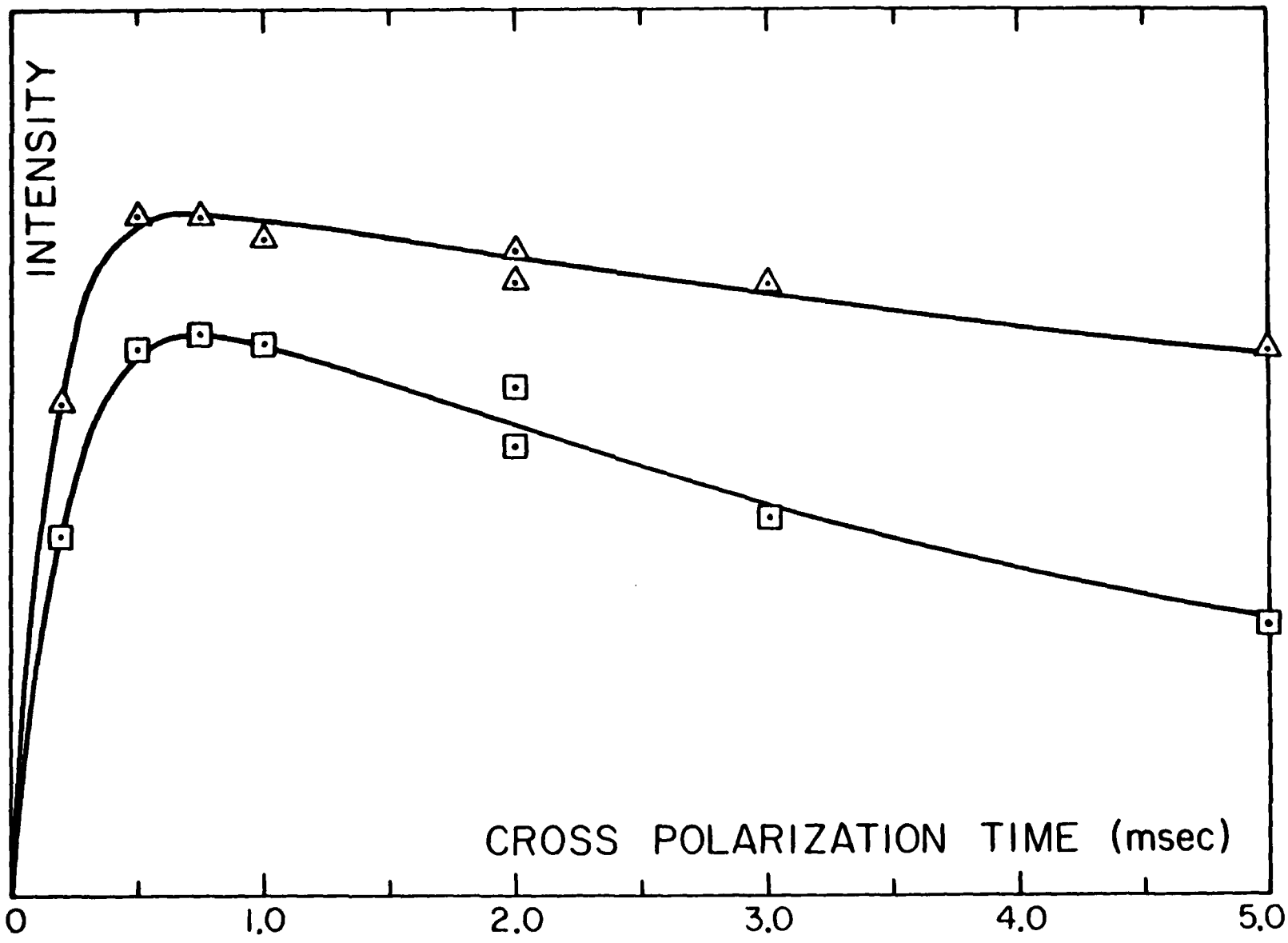
INTENSITY
CROSS POLARIZATION TIME (msec)
0
1.0
2.0
3.0
4.0
5.0

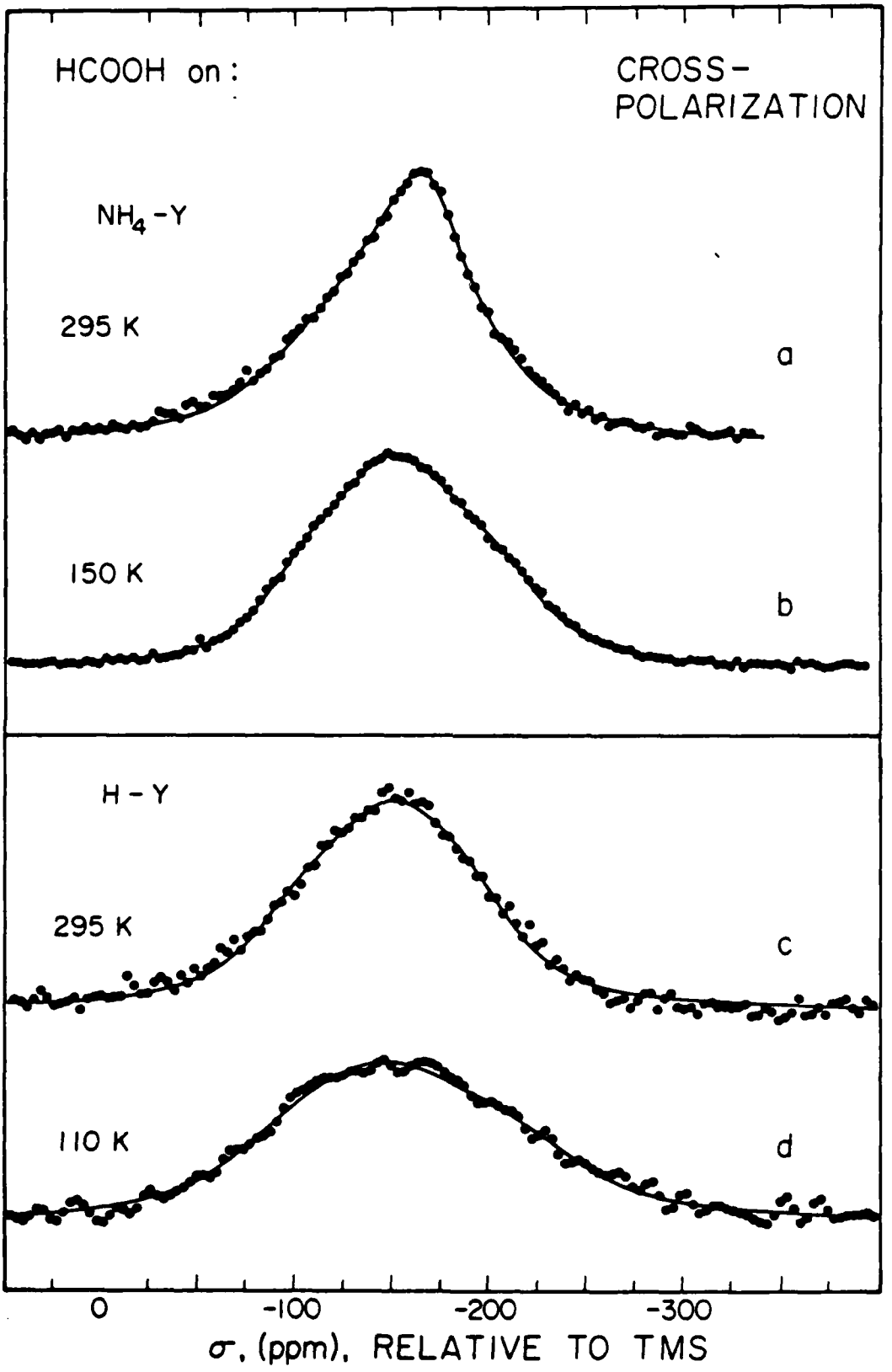
HCOOH on :
CROSS-
POLARIZATION
NH4-Y
295 K
a
150 K
b
H-Y
295 K
c
110 K
d
0
-100
-200
-300
σ, (ppm), RELATIVE TO TMS

Figure 7.

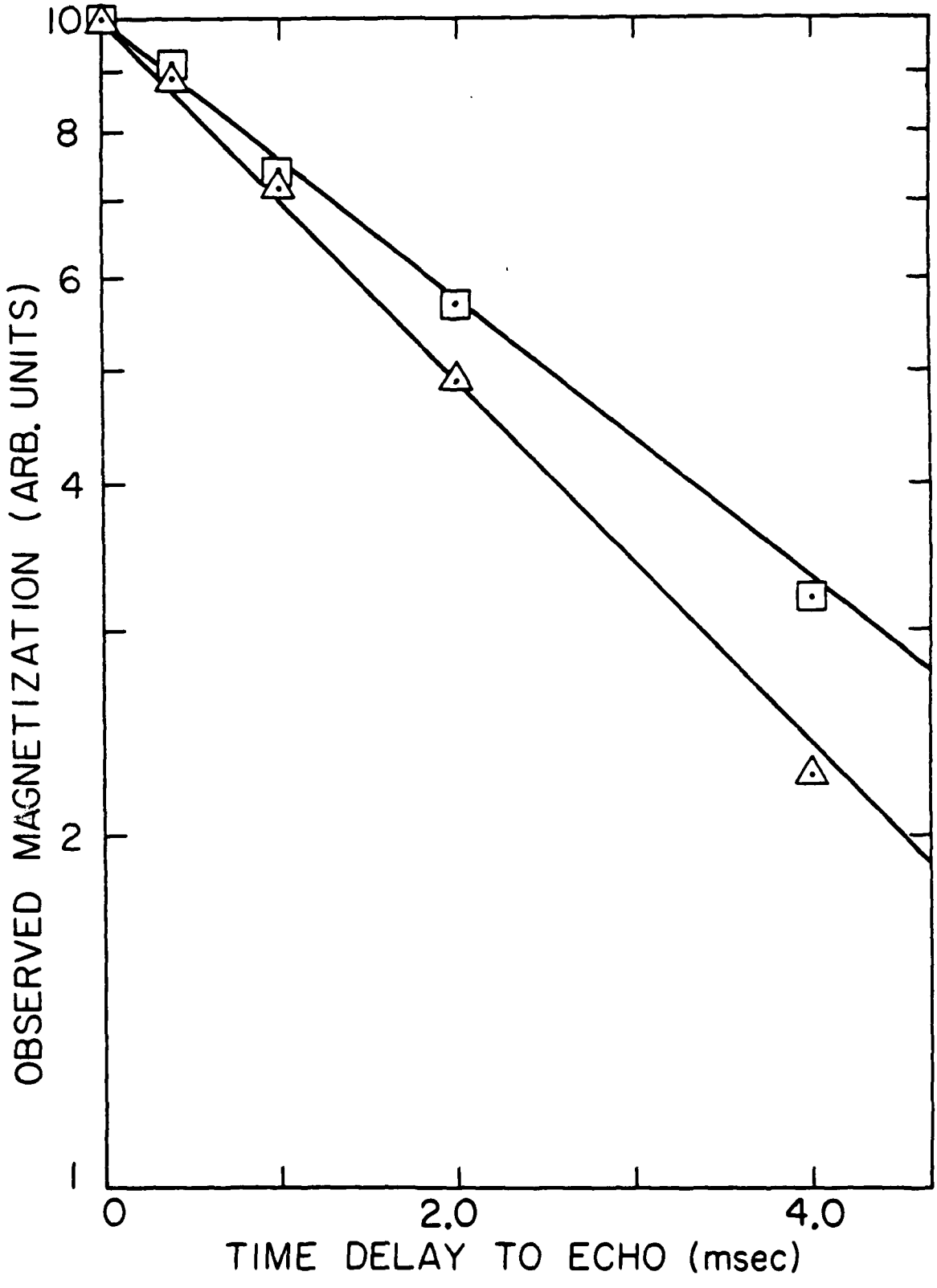
10
8
6
4
2
1
OBSERVED MAGNETIZATION (ARB. UNITS)
0
2.0
4.0
TIME DELAY TO ECHO (msec)

Figure 8

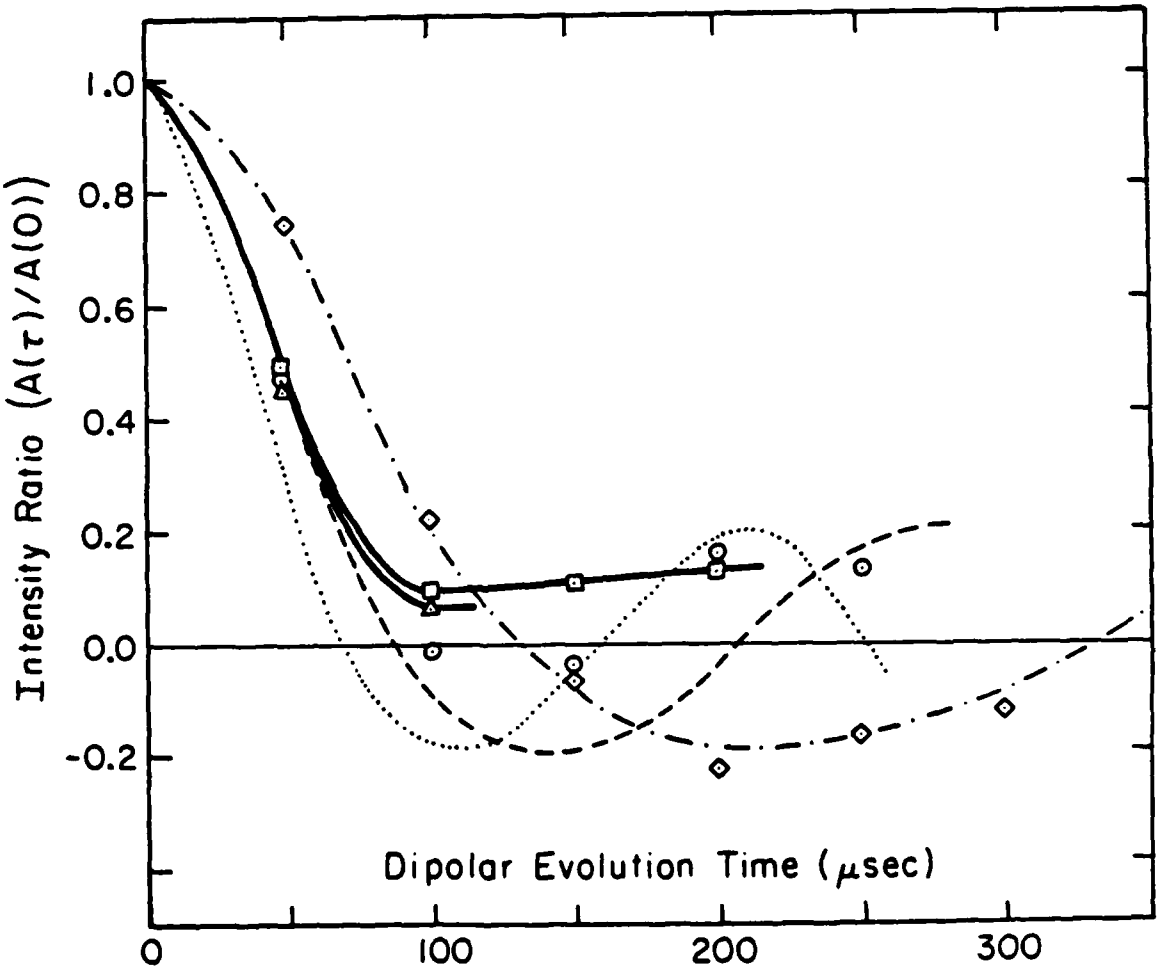
1.0
0.8
0.6
0.4
0.2
0.0
-0.2
Intensity Ratio (A(τ)/A(0))
0
100
200
300
Dipolar Evolution Time (μsec)

Figure

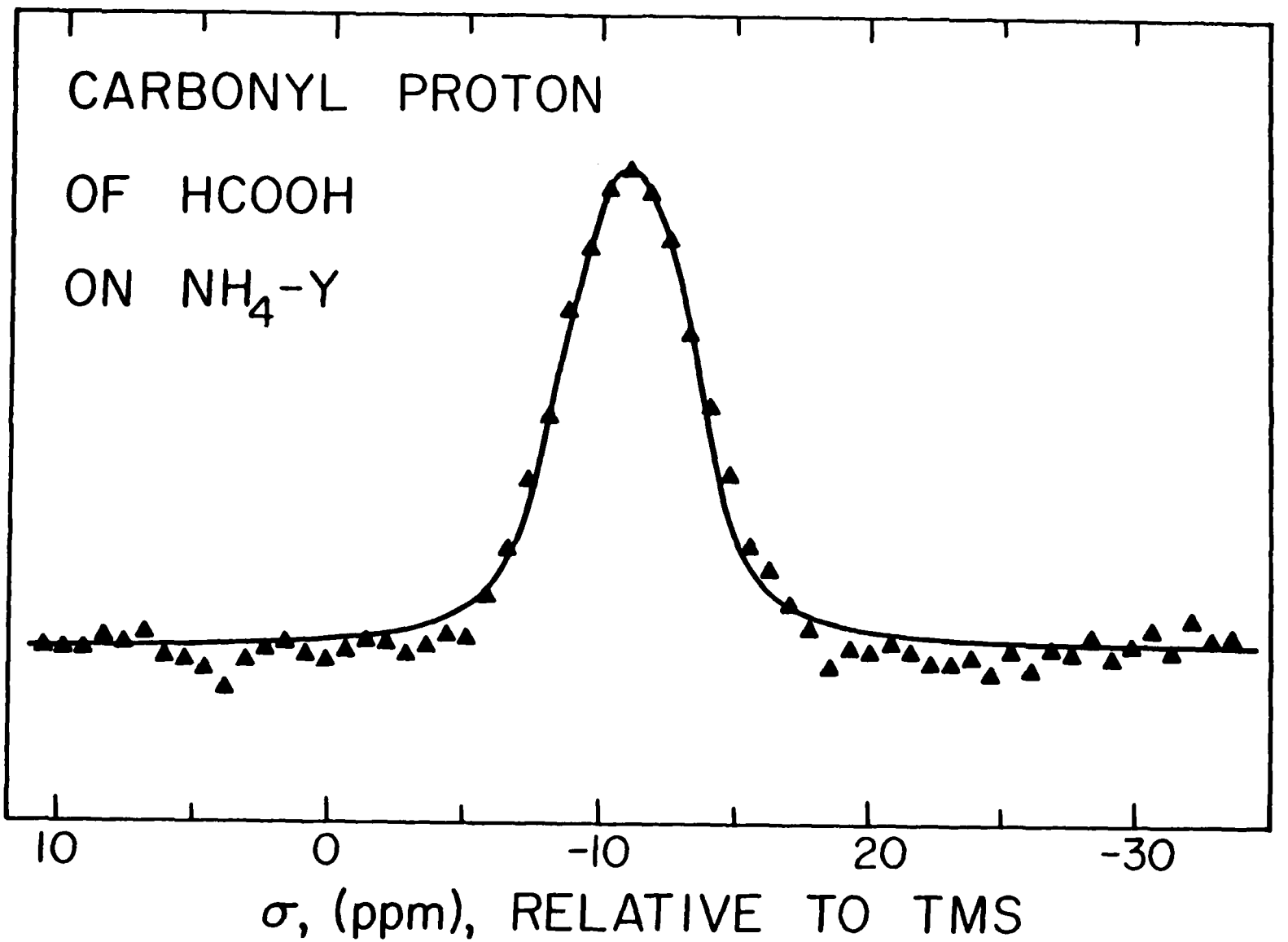
CARBONYL PROTON
OF HCOOH
ON NH_4-Y
10
0
-10
20
-30
σ, (ppm), RELATIVE TO TMS

Figure 10.